Journal of *Marine Science and Engineering*

MDPI

Review

A Comprehensive Review of an Underwater Towing Cable Array: A Discussion on the Dynamic Characteristics of the Towing Cable Array During the Outspread Process

Dapeng Zhang [1], Yangyang Luo [1,*], Yi Zhang [1], Yunsheng Ma [1], Keqiang Zhu [2] and Shengqing Zeng [1]

[1] Ship and Maritime College, Guangdong Ocean University, Zhanjiang 524005, China; zhangdapeng@gdou.edu.cn (D.Z.); zhangyi19492004@163.com (Y.Z.); yitcycyic@163.com (Y.M.); 18126369344@stu.gdou.edu.cn (S.Z.)
[2] Faculty of Maritime and Transportation, Ningbo University, Ningbo 315211, China; zhukeqiang@nbu.edu.cn
* Correspondence: luoyy@gdou.edu.cn

Abstract: Towing cable arrays have made significant contributions across various fields, and their outspread process is crucial for realizing their functionalities. However, research on the dynamic characterization of the outspread process of towed cable arrays lacks systematic organization. This paper reviews, organizes, and analyzes the outspread process of towing cable arrays, drawing on relevant models, case studies, and structural features. It ingeniously applies concepts from parachute outspread to the analysis of towing-cable-array deployment. The study systematically examines the deployment of towing cable arrays under varying cable lengths, wave conditions, and the interactions between line arrays. The goal is to integrate existing research on the outspread of towing cable arrays, addressing the gaps in the description of this process and providing a comprehensive analysis of the outspread characteristics under different conditions. Additionally, this paper identifies current limitations in this area and provides insights for future developments. Furthermore, it explores the potential application of AI to address these challenges. The aim of this paper is to contribute meaningfully to this field.

Keywords: towing cable array; outspread process; dynamic characterization; interactions

Citation: Zhang, D.; Luo, Y.; Zhang, Y.; Ma, Y.; Zhu, K.; Zeng, S. A Comprehensive Review of an Underwater Towing Cable Array: A Discussion on the Dynamic Characteristics of the Towing Cable Array During the Outspread Process. *J. Mar. Sci. Eng.* **2024**, *12*, 1880. https://doi.org/10.3390/jmse12101880

Academic Editors: Baiqiao Chen, Sheng Xu and Emre Uzunoglu

Received: 29 July 2024
Revised: 11 October 2024
Accepted: 18 October 2024
Published: 20 October 2024

1. Introduction

Conventional hull-mounted sonar systems have a limited detection range and are susceptible to interference from hull noise [1–4]. To improve detection, researchers have begun exploring the use of long transducer arrays towed at a distance from the hull. This led to the development of the towing-cable-array vibration system. The advantage of the towed system lies in its design, where the sonar receiver is embedded in a buoyant cable, keeping it away from the self-noise of the mothership [5,6]. This separation enables long-range detection [7,8]. In recent years, towed systems have been increasingly used across various fields due to their significant benefits. As illustrated in Figure 1, these fields primarily include seafloor topographic exploration [9,10], marine environment monitoring [11,12], marine rescue, protection of marine organisms [13,14], marine resources exploration [15,16], underwater archeology [17,18], and military applications [19–21]. As illustrated in Figure 2, the overall trend in the amount of literature on towing cable arrays has been increasing year by year, indicating a growing emphasis on this area. However, simulating the dynamic behavior and configuration of towed array cables is a challenging task. Compared to the traditional single-line array, the multi-branch towed-acoustic-array system addresses issues such as port and starboard ambiguity and target orientation during detection. Despite these advantages, the multi-branch system is more complex than the single-line array and is more prone to array distortion or even cable entanglement.

Figure 1. Areas of application for towing cable arrays.

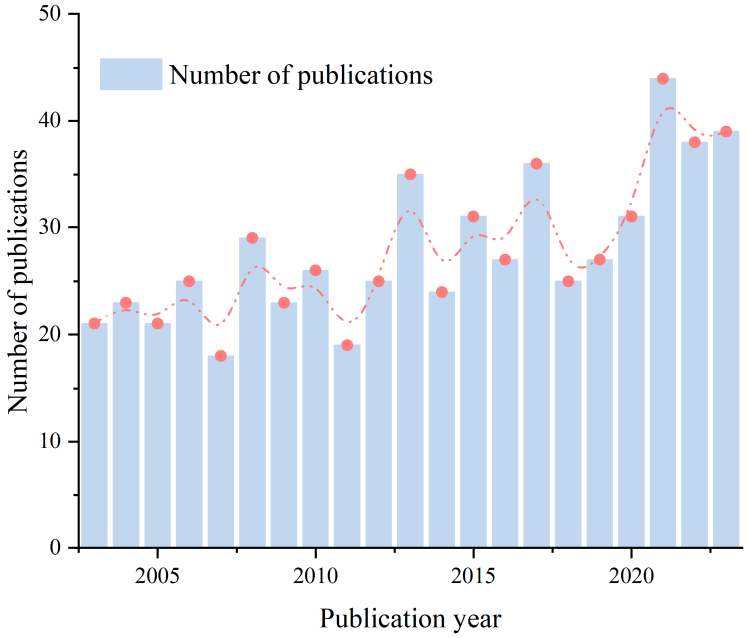

Figure 2. The number of published results about towing cable arrays in the Web of Science, from 2003 to 2023 [22].

It can be seen that there has been a lot of research on marine cables [23–26]. However, little research has been carried out on multi-branch towing cable arrays. There is a lack of systematic organization in the research on the outspread process of towing cable arrays. In the field of towing-cable-array dynamics, researchers typically rely on experimental methods and numerical simulation modeling. However, conducting experimental studies is often challenging and costly, resulting in a limited number of experimental cases on towing cable arrays. The modeling methods for towing cable arrays are primarily categorized into continuous and discrete approaches. While continuous models are not convenient for analytical solutions, they can be transformed into discrete equations, allowing for either pre-discretization followed by modeling or vice versa. Consequently, discrete methods have become the mainstream technology for solutions today. The process of towing-cable-array advection is complex, and most researchers simulate the study object as the towing cable array after completing the advection process. Therefore, this paper reviews, organizes, and analyzes the structural characteristics of the towing-cable-array outspread process based on relevant models, research cases, and the structural characteristics of towing cable arrays. This paper innovatively draws on aerospace research related to parachute outspread to

analyze the towing-cable-array outspread process. It systematically compiles, analyzes, and summarizes the characteristics of towing-cable-array outspread under varying cable lengths, wave conditions, and interference effects. The objective is to organize the existing research on towing-cable-array outspread, addressing gaps in the understanding of this process and providing a comprehensive overview in the field. Additionally, the exploration of how different interference conditions impact the towing-cable-array outspread process offers valuable insights for researchers. This paper also highlights some limitations in the field and proposes prospects for future development, including the potential application of AI to this problem. Ultimately, the aim of this paper is to make a meaningful contribution to the field.

2. Interesting Findings in Engineering Research

Through years of research on marine towing, the authors have uncovered an intriguing engineering problem. The multi-branch towing-cable-array sonar system is usually in a stable or quasi-stable state when it is in normal operation. This is because the working effectiveness and accuracy of the sonar system will be seriously affected when the motion state of the system changes too violently. The configuration of the multi-branch towed array and tension in the acoustic section of the towing cable array are two important indicators to judge whether the system is moving steadily or not. Generally, the actual configuration of the multi-branch towing cable array must be known, then the signal received by the hydrophone on the multi-branch towing cable array can be used for beamforming, and then the signal can be processed. The outspread process of the multi-branch towing cable array is the starting state of its normal operation, so the dynamic characteristics of the towing cable array during the outspread process will have a series of effects on the subsequent operation. However, the process of outspread has not received significant attention, and the relevant research in this area is poorly organized. To highlight this more intuitively, this paper presents a bibliometric analysis of studies published in the field of towing cable arrays from 2003 to 2023. This analysis is based on data from the Web of Science [22] database and conducted using Citespace [27] software.

Keywords can effectively highlight research hotspots [28–30], so this paper analyzes keyword emergence and frequency. Figure 3 and Table 1 present the keywords with the strongest citation bursts and the top 25 occurrences, respectively. In Figure 3, the red color indicates that a keyword was the focus of attention during a specific time period. It is evident that research in this field has gradually shifted from shallow waters to deeper regions, where sea conditions are more complex. To address these challenging environments, a comprehensive and systematic study of epipelagic processes is crucial. Additionally, more attention has been directed toward the application and performance of towing cable arrays in engineering, while less focus has been placed on the characteristics of multi-branch towing cable arrays.

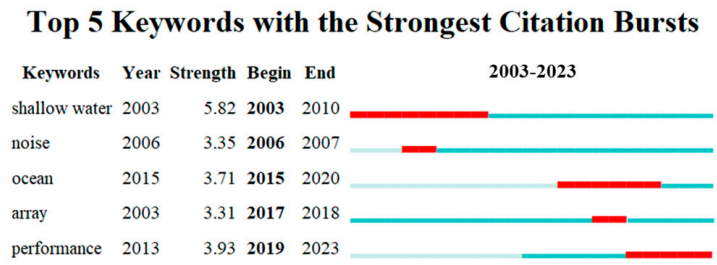

Figure 3. Emerging map of towing cable arrays.

Table 1. Keyword frequency table.

Count	Centrality	Keywords
42	0.21	Towed Array
40	0.11	Shallow Water
26	0.14	Array
24	0.24	Behavior
18	0.15	Arrays
17	0.1	Localization
13	0.07	Algorithm
13	0.01	Geoacoustic Inversion
13	0.08	Performance
12	0.07	Abundance
11	0.05	Array Signal Processing
11	0.03	Field
11	0.03	Noise
10	0.05	Inversion
9	0.02	Clicks
9	0.03	Ocean
8	0.01	Acoustic Data
8	0.04	Flow
8	0.07	Sea
7	0.04	Bottlenose Dolphins
7	0.04	Design
7	0.07	Tracking
6	0.02	Bottom
6	0.02	High-Resolution
6	0.08	Model

3. Mathematical Formulation

In the field of marine engineering, most studies on towing cable arrays focus on the state after the outspread is complete, with little attention given to the outspread process itself [31–35]. In contrast, the aerospace field provides extensive research on the outspread process of parachutes, which could offer valuable insights for the outspread of towing cable arrays [36–40]. As shown in Figure 4, despite differences in the medium and other factors, the outspread of parachutes and towing cable arrays share similar requirements regarding impact, stability, and material selection. This section presents two dynamics models relevant to the review, namely, one for the towing cable array after outspread in traditional ocean engineering field studies, and another for the parachute outspread process, which serves as a reference. The first kinetic model employs the lumped mass method [41–45] to discretize the tow cable in the array into a lumped mass model. Due to the fact that the cables are flexible components, their dynamic problems essentially include large deformation and hydrodynamic nonlinear problems. As the influence of equation system properties and the limitation of the flexible selection of boundary conditions, the applicability of finite element methods in solving marine cable problems is limited. The governing equations with nonlinear coefficients were first solved by the finite difference method, in which the equations are separated in space and time. Unlike the finite difference method, which solves the control equation from the perspective of the microelement, the lumped mass method directly starts from Newton's second law, approximates the marine cables as a series of nodes, which are connected by massless linear elastic elements, and regards the distributed forces such as gravity and hydrodynamic forces on the continuous pipeline as acting on the distribution nodes of the cable. The lumped mass method is more flexible than the finite difference method, so it seems to be a very economical and effective method to calculate the dynamic response of marine cables with the lumped mass method.

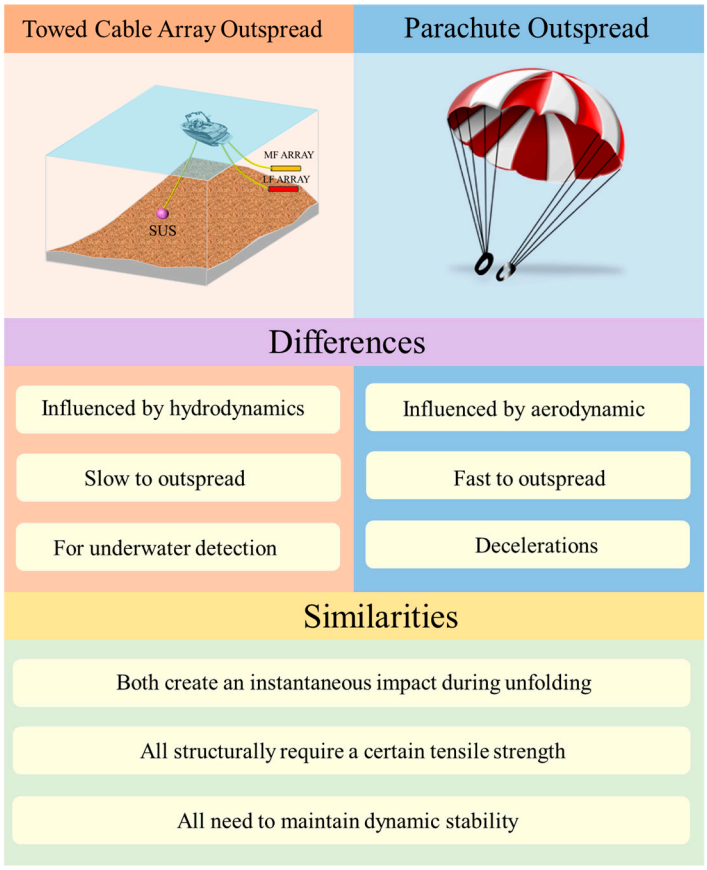

Figure 4. The similarities and differences between towing-cable-array outspread and parachute outspread.

3.1. Static Model of Towing Cable Array After Outspread

This paper establishes a coordinate system to clearly represent the heading angle and course direction of the towing-cable-array sonar system. It defines three systems, as follows: (1) the inertial coordinate system o−tnb, a fixed 3D Cartesian system where the origin is in the horizontal plane, with the t-axis pointing east and the n-axis north; (2) the towed-system motion coordinate system O−XYZ, which describes the positions of components within the sonar system, with its origin at the spacing hole and axes aligned with the bow and port directions; and (3) the local coordinate system o−xyz, fixed at the center of gravity of each sonar, detailing pitch and roll angles with axes oriented towards the bow and port. The paper uses the towing-cable-array motion coordinate system as the reference frame for numerical modeling and configuration display, necessitating coordinate conversion from the inertial frame for accurate calculations [46–48].

3.1.1. The Conversion of Relative Speed, Heading Angle, and the Course Direction of the Tugboat

The heading angle θ_{TC} is the angle measured clockwise from the north direction to the bow direction. The course direction angle θ_{CG} is measured clockwise to the absolute speed vector direction from the north direction, and the range of the course direction angle is [0°~360°]. The t-axis in the inertial system corresponds to the geographical east and the n-axis corresponds to the geographical north.

In the motion coordinate system of the towed system, the tugboat is taken as the reference frame without speed, then the actual speed and direction of the tugboat are expressed by the current speed [49,50]. Therefore, the current velocity V in the motion

coordinate system of the towed system is the relative speed v_r of the towed system in the inertial coordinate system, as follows:

$$V = v_r \tag{1}$$

The current direction angle θ_c (draft angle) is the difference between the course direction angle θ_{CG} and the heading angle θ_{TC}:

$$\theta_c = \theta_{CG} - \theta_{TC} \tag{2}$$

3.1.2. Coordinate Conversion of Pitch Angle, Roll Angle and Heading Angle of the Connecting Frame

The pitch angle and roll angle of the connecting frame are the angles between the *x*-axis and *y*-axis of the local coordinate system of the connecting frame and the o-tn surface of the inertial system, which are the same as those in the motion coordinate system of the towed system.

The course direction angle ψ_0 of the connecting frame is measured clockwise from the n-axis positive direction of the inertial system to the *x*-axis positive direction of the local coordinate system of the connecting frame. The heading angle of the connecting frame in the towed-system motion coordinate system is the angle between the positive direction of the *X*-axis and the positive direction of the *x*-axis in the local coordinate system of the towed-system motion coordinate system:

$$\Psi = \psi_0 - \theta_{TC} \tag{3}$$

The coordinate positions in the towed-system motion coordinate system can be obtained by a matrix transformation of the initial coordinates of the bottom end points of the connecting frame [51,52]. The roll angle, pitch angle, and heading transformation matrices of the connecting frame are as follows:

$$X_{ch} = \begin{bmatrix} 1 & 0 & 0 \\ 0 & \cos\varphi & \sin\varphi \\ 0 & -\sin\varphi & \cos\varphi \end{bmatrix} \tag{4}$$

$$Y_{ch} = \begin{bmatrix} \cos\theta & 0 & \sin\theta \\ 0 & 1 & 0 \\ -\sin\theta & 0 & \cos\theta \end{bmatrix} \tag{5}$$

$$Z_{ch} = \begin{bmatrix} \cos\psi & \sin\psi & 0 \\ -\sin\psi & \cos\psi & 0 \\ 0 & 0 & 1 \end{bmatrix} \tag{6}$$

The initial coordinate of the bottom end point of the connecting frame in the towed-system motion coordinate system is (i_0, j_0, k_0). The new coordinate (i, j, k) of the bottom end point of the connecting frame is obtained by matrix transformation.

$$(i, j, k) - (i_0, j_0, k_0) M_{ch} \tag{7}$$

where

$$M_{ch} = Z_{ch} X_{ch} Y_{ch} \begin{bmatrix} \cos\theta\cos\psi & \sin\psi & \sin\theta\cos\psi \\ -\cos\theta\sin\psi & \cos\psi & -\sin\psi\sin\theta \\ -\sin\varphi & 0 & \cos\theta \end{bmatrix} \tag{8}$$

The connection frame is an isosceles triangular support located at the top of the towing-cable-array sonar to connect the towing cable and the connection chains [53–55]. Therefore, by determining the coordinates of the connecting frame, the underwater configuration of the towing-cable-array sonar can be obtained.

The diagram of the towing cable under the spacing hole in the towed motion coordinate system is shown in Figure 5. The coordinate of X-axis X_{f_0} and Y-axis Y_{f_0} at the end of the towing cable can be obtained from the current direction and the length that has been lowered.

$$X_{f_0} = l_{cable} \sin \theta_c \tag{9}$$

$$Y_{f_0} = l_{cable} \cos \theta_c \tag{10}$$

where l_{cable} is the projection length of the towing cable in XOY plane.

$$l_{cable} = \sqrt{L_{cable} - H_{f_0}^2} \tag{11}$$

$$L_{cable} = L_{out} - H_W + H_h \tag{12}$$

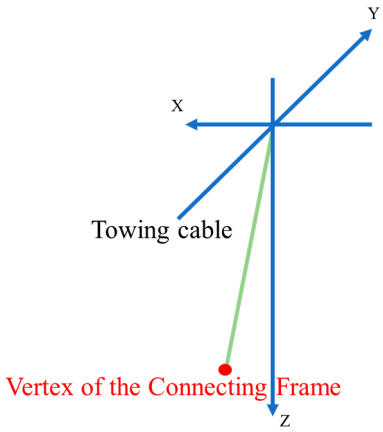

Figure 5. A diagram of the towing cable below the spacing hole.

L_{cable} is the length under the spacing hole, L_{out} is the cable length that has been lowered, and HW is the elevation between the winch center and the sea level.

As the top end of the connecting frame is connected to the end of the towing cable, the height from the end of the towing cable to the spacing hole is equal to the Z-axis coordinate Z_{f_0} at the top of the connecting frame, which can be expressed as:

$$Z_{f_0} = H_{f_0} = H_{top} - l_{e-l} + H_h \tag{13}$$

where H_{f_0} is the height from the top of the connecting frame (the end of the towing cable) to the spacing hole; H_{top} is the depth of the top mounted sonar; le-t is the distance from the top end to the bottom end of the towing cable; and H_h is the height from the spacing hole to the sea level.

After the coordinate $(X_{f_0}, Y_{f_0}, Z_{f_0})$ of the top point of the connecting frame is obtained, when the heading, pitch angle, and roll angle are all 0° are calculated according to the dimensions of the connecting frame members, the coordinates (X_{ff}, Y_{ff}, Z_{ff}) and (X_{fb}, Y_{fb}, Z_{fb}) of the front end and the bottom end of the connecting frame. Substitute the coordinates into Equation (7); then, the coordinates $(X_{ff_0}, Y_{ff_0}, Z_{ff_0})$ and $(X_{fb0}, Y_{fb0}, Z_{fb0})$ of the front end and the bottom end of the connecting frame are obtained:

$$\left(X_{fb0}, Y_{fb0}, Z_{fb0}\right) = \left(X_{fb}, Y_{fb}, Z_{fb}\right) M_{ch} \tag{14}$$

$$\left(X_{ff_0}, Y_{ff_0}, Z_{ff_0}\right) = \left(X_{ff}, Y_{ff}, Z_{ff}\right) M_{ch} \tag{15}$$

3.1.3. The Calculation of the Connecting Chain

The connecting chains and mounts on both sides of a segment of a towing cable array are selected and their torsional configurations are shown in Figure 6.

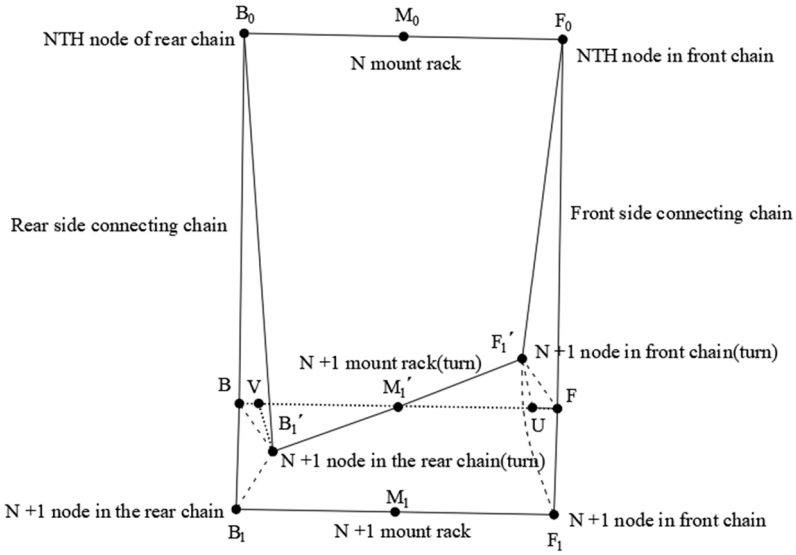

Figure 6. Torsional configurations of the connecting chain and mounts.

Before the mount rack rotates, the segmented configuration of the towed-array cable is the parallelogram $B_0B_1F_0F_1$. The rotated segmented configuration is a spatial quadrilateral $B_0\ B_1'F_1'F_0$ with equal opposite sides.

$\angle BM_1'B_1'$ and $\angle FM_1'F_1'$are the difference between N mount rack and N + 1 mount rack, as follows:

$$\angle BM_1'B_1' = \angle FM_1'F_1' = \theta_{n+1TC} - \theta_{nTC} \tag{16}$$

where $\theta_n + 1$ is the relative course direction of N + 1 mount rack; and θ_{n+1TC} and θ_{nTC} are the course directions of N + 1 mount rack and N mount rack, respectively.

$$BB_1' = FF_1' = \sqrt{(M_1'B)^2 + (B_1M_1')^2 - 2M_1'B \cdot B_1M_1' cos\angle BM_1'B_1'} \tag{17}$$

The connecting chain and the mount rack are considered to be perpendicular to each other when it is not turned, so the length of B0B and F0F can be calculated as follows:

$$\angle BM_1'B_1' = \angle FM_1'F_1' = \theta_{n+1} = \theta_{n+1TC} - \theta_{nTC} \tag{18}$$

Since the midpoint line M_0M_1' of the n + 1 mount is parallel to the two connecting chains before rotation, the coordinates (X_{M1}', Y_{M1}', Z_{M1}') of the midpoint M_1' of the n + 1 mount after rotation can be represented by the midpoint M_0 of the N mount and the vector $\overrightarrow{B_0B}$:

$$(X_{M_1}, Y_{M_1}, Z_{M_1}) = (X_{M_0}, Y_{M_0}, Z_{M_0}) + \left|\overrightarrow{B_0B}\right|\vec{m} \tag{19}$$

where the vector $\vec{m}$ is the unit direction vector of the vector $\overrightarrow{B_0B}$, which is in the same direction as that of the vector arrow from the top of the connecting frame to the middle point of the bottom edge.

The end-point coordinates of B_1' and F_1' on both sides of the mount after rotation can be obtained by translating the point coordinates M1′ along the vectors $\overrightarrow{M_1'B_1'}$ and $\overrightarrow{M_1'F_1'}$. Since it is difficult to obtain the vectors $\overrightarrow{M_1'B_1'}$ and $\overrightarrow{M_1'F_1'}$ directly through coordinates, they can be expressed by the vectors $\overrightarrow{M_1'V}$, $\overrightarrow{VB_1'}$, $\overrightarrow{M_1'U}$ and $\overrightarrow{UF_1'}$

$$\overrightarrow{M_1'B_1'} = \overrightarrow{M_1'V} + \overrightarrow{VB_1'} \tag{20}$$

$$\overrightarrow{M_1'F_1'} = \overrightarrow{M_1'U} + \overrightarrow{UF_1'} \tag{21}$$

Since the connecting chain is connected to the connecting rack, in the towed-system motion coordinate system, the connecting chain top end-point coordinate is the connecting rack bottom end-point coordinate:

$$\left(X_{cb_0}, Y_{cb_0}, Z_{cb_0}\right) = \left(X_{fb_0}, Y_{fb_0}, Z_{fb_0}\right) \tag{22}$$

$$\left(X_{cf_0}, Y_{cf_0}, Z_{cf_0}\right) = \left(X_{ff_0}, Y_{ff_0}, Z_{ff_0}\right) \tag{23}$$

where $\left(X_{cf_0}, Y_{cf_0}, Z_{cf_0}\right)$ and $\left(X_{cb_0}, Y_{cb_0}, Z_{cb_0}\right)$ are the top coordinates of front and rear connecting chains, respectively.

3.1.4. The Force of Each Part of the Towing-Cable-Array System

(1) Gravity and buoyancy

The buoyancy F_{fwet} of the towing cable in water can be expressed as:

$$F_{fwet} = \frac{1}{4}\pi d_{cable}^2 (L_{out} - H_w)\rho g \tag{24}$$

where d_{cable} is the diameter of the towing cable; L_{out} is the lower length of the towing cable; H_w is the elevation from the center of the winch to the sea level; ρ is the density of sea water; g is the gravitational acceleration.

The gravity Gout of the towing cable in water can be expressed as:

$$G_{out} = L_{out} m_{cable} g \tag{25}$$

where m_{cable} is the linear density of the towing cable.

The weight of the towing cable in water can be expressed as:

$$G_{cable} = L_{out} m_{cable} g - \frac{1}{4}\pi d_{cable}^2 (L_{out} - H_w)\rho g \tag{26}$$

The weight G_F of the connecting frame of the towing cable array in water can be expressed as:

$$G_F = M_F g - \frac{1}{4}\pi d_F^2 L_F \rho g \tag{27}$$

where M_F is the mass of the connecting frame; dF is the diameter of the connecting frame; and L_F is the total length of the connecting frame.

(2) Hydrodynamic load

Let the water velocity be $\vec{J} = J_1\vec{\tau} + J_2\vec{n} + J_3\vec{b} = J_X\vec{i} + J_Y\vec{j} + J_Z\vec{k}$ The velocity of the cable with respect to the water in the Lagrangian coordinate system is:

$$\begin{cases} v_{1r} = u - J_1 \\ v_{2r} = v - J_2 \\ v_{3r} = w - J_3 \end{cases} \tag{28}$$

Since both ends of the microelement are connected to adjacent microelements, without direct contact or interaction with the water, the tangential upward added mass force and dynamic Archimedean force are zero. Therefore, the hydrodynamic loading is limited to the drag force.

According to Morison's equation, the expression for tangential resistance is:

$$\overrightarrow{F_{dr,t}} = -\frac{1}{2}\rho_w d_1 \pi C_{dr} v_{1r} |v_{1r}| \vec{\tau} \tag{29}$$

Hydrodynamic loads in the plane perpendicular to the cable include drag, additional mass forces, and dynamic Archimedean forces. The expression for the drag force is as follows:

$$\begin{cases} \overrightarrow{F_{dr,n}} = -\frac{1}{2}\rho_w d_1 C_{dp} v_{2r}\sqrt{v_{2r}^2 - v_{3r}^2}\,\vec{n} \\ \overrightarrow{F_{dr,b}} = -\frac{1}{2}\rho_w d_1 C_{dp} v_{3r}\sqrt{v_{2r}^2 - v_{3r}^2}\,\vec{b} \end{cases} \tag{30}$$

The dynamic Archimedean force is independent of the acceleration of the cable element and is determined by the acceleration of the currents $\dot{J}_2$ and $\dot{J}_3$ with vector expressions as follows:

$$\begin{cases} \overrightarrow{F_{dA,n}} = \rho_w \frac{\pi d^2}{4(1+e)}\dot{J}_2\vec{n} \\ \overrightarrow{F_{dA,b}} = \rho_w \frac{\pi d^2}{4(1+e)}\dot{J}_3\vec{b} \end{cases} \tag{31}$$

The added mass force is generated by the acceleration of the fluid around the cable element and depends on the added mass of the cross-section, as well as the acceleration of the cross-section relative to the surrounding fluid in the $\dot{v}_{2r}$ and $\dot{v}_{3r}$ directions.

$$\begin{cases} \overrightarrow{F_{am,n}} = \frac{m_a}{(1+e)}\dot{v}_{2r}\vec{n} \\ \overrightarrow{F_{am,b}} = \frac{m_a}{(1+e)}\dot{v}_{3r}\vec{b} \end{cases} \tag{32}$$

(3) Drag force

The Morison equation [56–58] is used to calculate the drag force of the towing cable in this paper. When the force balance equation of the connecting frame is established, the drag force of the towing cable needs to be decomposed to the X, Y and Z axis components.

The connecting frame is an isosceles triangular support, which consists of three members with circular cross-sections. Due to the different normal speeds of each member, its drag force is made up of three parts, as follows:

$$\overrightarrow{F_f} = \left(\overrightarrow{f_{f_b}} + \overrightarrow{f_{ff}}\right)l_f + \overrightarrow{f_{fB}}l_{fB} \tag{33}$$

where $\overrightarrow{f_{ff}}$, $\overrightarrow{f_{f_b}}$, $\overrightarrow{f_{fB}}$ are the drag force vectors per unit length of members on both sides and bottom of the connecting frame, respectively; and l_{fB} is the length of the bottom member of the connecting frame.

In the towed-system motion coordinate system, the relative velocity of the connecting frame is equal to the current velocity [59,60]. Then, the normal velocity of each member of the connecting frame can be expressed as:

$$V_{ff} = V\cos\alpha_{ff} = V\cos\left(-\frac{1}{2}\beta_{frame} + \alpha_{frame}\right) \tag{34}$$

$$V_{fb} = V\cos\alpha_{fb} = V\cos\left(\frac{1}{2}\beta_{frame} + \alpha_{frame}\right) \tag{35}$$

$$V_{fB} = V\cos\alpha_{fB} = V\cos\left(90^\circ - \alpha_{frame}\right) \tag{36}$$

where V_{ff}, V_{fb}, V_{fB} are the normal velocities of the front, rear, and bottom members of the connecting frame, respectively; α_{ff}, α_{fb}, α_{fB} are the pitch angles of the front, rear, and bottom members of the connecting frame, respectively; β_{frame} is the pitch angle of the front members of the connecting frame, and α_{frame} is the pitch angle of bottom members of the connecting frame.

By substituting V_{ff}, V_{fb} and V_{fB} into the Morison equation, the drag force of the front, rear, and bottom members of the connecting frame can be obtained.

(4) The tension of the towing cable at the spacing hole

The force of the towing cable at the spacing hole is shown in Figure 7. The towing cable is subjected to the tension T_W of the winch, the wall pressure F_{hole} of the spacing hole, the gravity G_{cable0} of the towing cable above the spacing plate, and the tension T_{co} of the towing cable below the spacing plate at the spacing hole. It can be seen that the winch tension and the gravity of the upper towing cable are both along the *Z*-axis direction, and the *Z*-axis component of the tension of the lower towing cable is equal to the resultant force of the winch tension and the gravity of the upper towing cable.

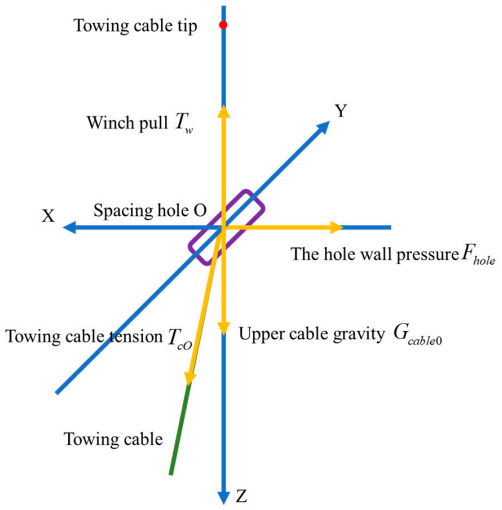

Figure 7. The force of the towing cable at the spacing hole.

Then, the following equation can be obtained:

$$T_{co}cos\propto_{cable} + G_{cable0} - T_W = 0 \tag{37}$$

Then, the tension TCO of the towing cable at the spacing hole can be obtained:

$$T_{co} = \frac{T_W - G_{cable0}}{cos\alpha_{cable}} \tag{38}$$

(5) Tension of the towing cable at the towed end A

The schematic diagram of the overall force of the towing cable is shown in Figure 8. If the part of the towing cable under the spacing plate is considered as a whole, the force on the towing cable can be shifted to its center of gravity. Since the horizontal component of the towing cable tension is always opposite to the direction of the resistance, the forces acting on the towing cable can be decomposed along the *Z*-axis and parallel to the XOY plane, and the force balance equation for the towing cable under the spacing plate is obtained as follows:

$$T_{co}cos\alpha_{cable} - T_{cAz} - G_{cable} - F_{fcablez} = 0 \tag{39}$$

$$T_{co}sin\alpha_{cable} - T_{cAXOY} + F_{fcableXOY} = 0 \tag{40}$$

Then, the components of the tension at end A of the towing cable along the *Z*-axis and in the XOY plane can be obtained:

$$T_{co}sin\alpha_{cable} - T_{cAXOY} + F_{fcableXOY} = 0 \tag{41}$$

$$T_{cAXOY} = (T_{co}cos\,\alpha_{cable} - G_{cable}) \tag{42}$$

Then, the tension at end A of the towing cable can be written as:

$$T_{cA} = \sqrt{T_{cAz}^2 + T_{cAXOY}^2} \tag{43}$$

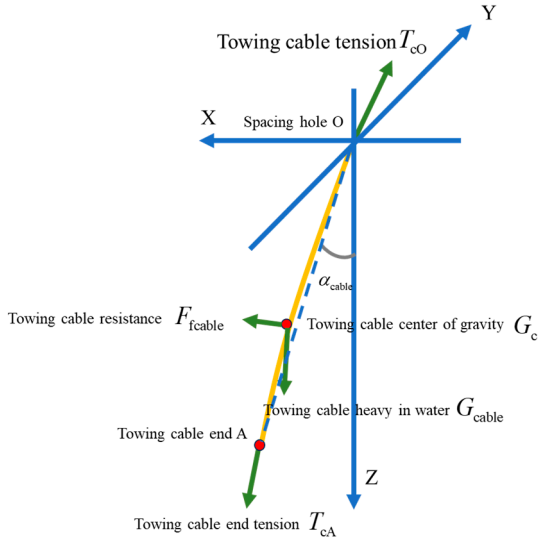

Figure 8. A schematic diagram of the overall force of the towing cable.

(6) Equilibrium equation of the towing cable and the connecting frame

Figure 9 is the force analysis of the towing cable and the connecting frame, it can be seen that the connecting frame is subjected to forces in different directions. Therefore, when solving the top load of the connecting chain, it is necessary to decompose the forces acting on the towing-cable connecting frame along the X, Y and Z axes of the towed-system motion coordinate system as follows:

$$T_{cAX} - F_{Cbx} - F_{Cfx} - F_{fx} = 0 \tag{44}$$

$$T_{cAY} - F_{Cby} - F_{Cfy} - F_{fy} = 0 \tag{45}$$

$$T_{cAZ} - F_{CbZ} - F_{Cfz} - G_F = 0 \tag{46}$$

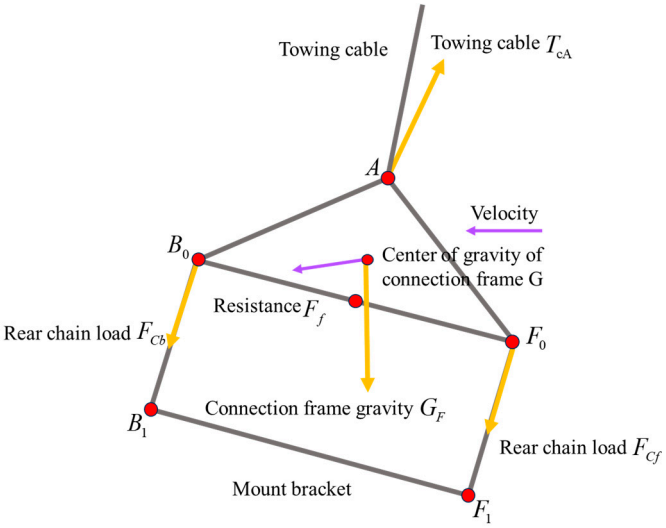

Figure 9. A force analysis of the towing cable and the connecting frame.

The tension at end A of the towing cable is obtained in the previous section and the direction of tension is unknown. The included angle between the tension at the A end of the towing cable and the negative direction of the *X*-axis is $\propto_{X_{cA}}$, and the positive direction is clockwise. The included angle with the negative direction of *Z*-axis is $\propto_{Z_{cA}}$; then, the

components of the towing cable end tension T_{cA} in the X, Y, Z axis directions are shown as follows:

$$T_{cAX} = T_{cA} sin \propto_{zcA} cos \propto_{XcA} \tag{47}$$

$$T_{cAY} = T_{cA} sin \propto_{ZcA} sin \propto_{XcA} \tag{48}$$

$$T_{cAZ} = T_{cA} cos \propto_{ZcA} \tag{49}$$

The loads of the connecting chain on both sides are equal. The load on the top of the connecting chain on the rear side is Fc; then, we can obtain the following equation:

$$\left|\overrightarrow{F_{Cf}}\right| = \left|\overrightarrow{F_{Cb}}\right| = F_c \tag{50}$$

If the node coordinates of the connecting chain are known, the components of the loads F_{Cf}, F_{Cb} acting on both sides of the connecting frame in the directions of X, Y, and Z axes can be represented by the vectors $\overrightarrow{B_0B_1}$ and $\overrightarrow{F_0F_1}$:

$$(F_{CbX}, F_{CbY}, F_{CbZ}) = |F_{Cb}| \frac{\overrightarrow{B_0B_1}}{\left|\overrightarrow{B_0B_1}\right|} \tag{51}$$

$$\left(F_{CfX}, F_{CfY}, F_{CfZ}\right) = \left|F_{Cf}\right| \frac{\overrightarrow{F_0F_1}}{\left|\overrightarrow{F_0F_1}\right|} \tag{52}$$

where F_{CbX}, F_{CbY}, F_{CbZ} and F_{CfX}, F_{CfY}, F_{CfZ} are the components of X, Y, and Z axes of the front and rear connecting chain loads.

By substituting Equations (41)–(46) into Equations (38)–(40), a set of three-component equations can be obtained. By solving the set of equations, the load of the joint at the top of the connecting chain on both sides can be obtained.

3.2. A Dynamic Outspread Model with Reference Significance

Parachute outspread is a complex process [61–63], comparable to the outspread of towing cable arrays. Consequently, parachute outspread is vulnerable to phenomena such as "Linesail" [64,65], which can have numerous adverse effects. The aerospace field has extensively studied the parachute outspread process, making it a valuable reference for understanding the outspread of towing cable arrays. In this section, selected research by Zhang [66] and Wang [67] from the National University of Defence Technology is reviewed for analytical studies.

In Zhang's study, as illustrated in Figure 10, the parachute system is modeled as a series of rigid chain segments connected by rotating joints. Each rigid chain segment represents a portion of the suspension system. The mass of each rigid body within the system is distributed across its two endpoints, which are treated as nodes of the suspension system. The orientation of the chain segments is denoted by the angle θ_n.

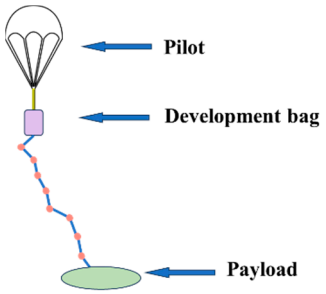

Figure 10. The parachute system.

The Newton–Euler method is employed to derive the acceleration of the nodes in the system, considering aerodynamic, gravitational, and other forces in the calculations.

(1) Calculation of velocity and acceleration

For a node m_n in the system, its velocity and acceleration in the X and Y directions is given by:

$$v_x^n = v_x^{n-1} - \dot{\theta} L_n sin\theta_n \tag{53}$$

$$v_y^n = v_y^{n-1} - \dot{\theta} L_n cos\theta_n \tag{54}$$

$$a_x^n = a_x^{n-1} - \ddot{\theta}_n L_n sin\theta_n - \dot{\theta}_n^2 L_n cos\theta_n \tag{55}$$

$$a_y^n = a_y^{n-1} - \ddot{\theta}_n L_n cos\theta_n - \dot{\theta}_n^2 L_n sin\theta_n \tag{56}$$

(2) Equilibrium equations of forces

According to Newton's second law, the equilibrium equation of force on the mass point m_n is:

$$m_n a_x^n = T_{n+1} cos\theta_{n+1} - T_n cos\theta_n + Q_x^n + m_n g \tag{57}$$

$$m_n a_y^n = T_{n+1} sin\theta_{n+1} - T_n sin\theta_n + Q_y^n \tag{58}$$

In the equation, g represents the acceleration due to gravity. Q_x^n and Q_y^n denote the aerodynamic forces acting on the nth link.

(3) Recursive constraint algorithm

In order to solve for the constraint of the system, a recurrence relation is established:

$$\begin{bmatrix} T_{n+1} \\ \ddot{\theta}_n \end{bmatrix} = \begin{bmatrix} cos\theta_{n+1} & m_n L_n sin\theta_n \\ sin\theta_{n+1} & -m_n L_n cos\theta_n \end{bmatrix}^{-1} [K_n] \tag{59}$$

Here:

$$[K_n] = m_n \left(\begin{bmatrix} a_x^{n-1} \\ a_y^{n-1} \end{bmatrix} + \begin{bmatrix} -\dot{\theta}_n^2 L_n cos\theta_n \\ -\dot{\theta}_n^2 L_n sin\theta_n \end{bmatrix} \right) - \begin{bmatrix} m_n g \\ 0 \end{bmatrix} + \begin{bmatrix} T_n cos\theta_n \\ T_n sin\theta_n \end{bmatrix} - \begin{bmatrix} Q_x^n \\ Q_y^n \end{bmatrix} \tag{60}$$

Using this recurrence relation, all the constraint forces T_n can be solved for to determine the acceleration of each node.

(4) Solving for Separation Velocity

For the separation speed of the system $\dot{L_n}$, construct the linear function:

$$fun(x) = \alpha x + \beta - F_c \tag{61}$$

The true separation velocity is obtained by finding the zeros in three iterations:

$$\ddot{L_1} = \frac{\ddot{L_1^1} fun\ddot{L_1^2} - \ddot{L_1^2} fun\ddot{L_1^1}}{fun\ddot{L_1^1} - fun\ddot{L_1^2}} \tag{62}$$

In Wang's study, the parachute suspension was simulated using a mass-spring-damper model. During the outspread process, the suspension line continuously extends from the parachute bag and moves with the system, as illustrated in Figure 11.

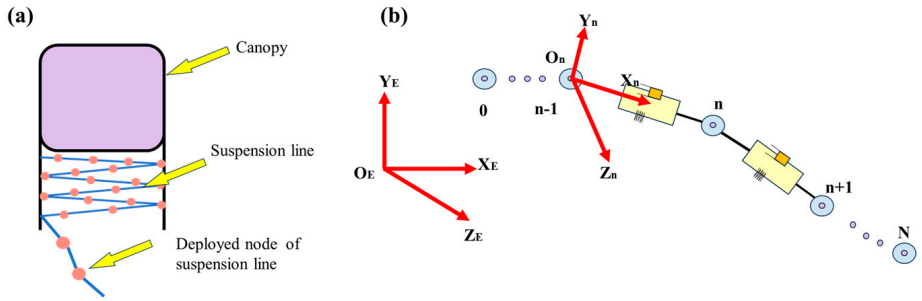

Figure 11. (**a**) A sketch of the outspread model of the suspension line and the canopy. (**b**) The mass-spring-damper model.

Therefore, a pullout model is typically used to represent this behavior. When the distance between the last node and the next neighboring node in the umbrella pack exceeds the original length, a new node is pulled out, and the dynamics equation is:

$$m_i \ddot{r}_i = \vec{F}_{ai} + \vec{F}_r + \vec{F}_{gi} + \vec{F}_{ti} + \vec{F}_{tie} \tag{63}$$

where $\vec{F}_{ai}$, $\vec{F}_r$, $\vec{F}_{gi}$, $\vec{F}_{ti}$ and $\vec{F}_{tie}$ represent the aerodynamic force, friction force, gravitational force, tension, and constraint force of the i-th suspension node, respectively. $\vec{F}_{tie}$ is ignored when the node is not constrained. The constraint force of the proposed node using the line spring model, $\vec{F}_{tie}$, is given by:

$$\vec{F}_{tie} = \begin{cases} k\varepsilon & 0 < \varepsilon < \varepsilon_{max} \\ 0 & \varepsilon \leq 0 \; or \; \varepsilon > \varepsilon_{max} \end{cases} \tag{64}$$

where ε is the strain of the constraint suspension and ε_{max} is the maximum permitted strain.

The outspread process of a towing cable array shares similarities with the outspread of a parachute, as both involve nonlinear deformations driven by fluid forces. However, significant differences arise due to their distinct environments. Towing cable arrays operate underwater, where they are influenced by complex hydrodynamic forces and buoyancy, whereas parachutes outspread in the atmosphere under aerodynamic forces. These environmental distinctions lead to differences in structural design, dynamic response, and control strategies. In addition, towing cable arrays must account for non-uniform load distributions caused by water currents and the dynamic coupling effects of multi-branch systems. These challenges impose higher demands on the research of towing cable arrays, particularly in the analysis of their nonlinear hydrodynamic behavior and the stability of their working attitude.

4. Factors Affecting Towing-Cable-Array Outspread

Through the authors' extensive exploration of the field and a thorough review of existing research, it is evident that several factors influence the outspread process of towing cable arrays. These factors include towline length, wave impact, alignment spacing, tip-drawing dynamics, and tension fluctuations.

4.1. Towline Length

The length of the tow cable is a crucial feature of the towing cable array, significantly influencing the outspread process in terms of dynamic response and complexity. The length of the towing cable is a crucial feature of the towing cable array, as it significantly affects the outspread process, influencing the dynamic response, complexity, and spatial orientation of the array.

The ratio $\frac{R}{L}$ of the total length of the towing cable to the radius of turning is a crucial parameter for describing the dynamics of a motorized towing system [68]. However, it

appears that the primary focus has been on the variation in the radius of gyration, neglecting the impact of different cable lengths [69–71]. Kamman and Huston [72] provide a detailed modeling and analysis methodology for variable-length towing and tethered cable systems, effectively capturing their complex dynamic behavior. As shown in Figure 12 of their study, three cable length increases—50 ft, 100 ft, and 150 ft—were selected to observe the changes in the pitch angle of the towed body over time. The results indicate that the pitch angle of the tractor initially increases with the extension of the cable, then gradually decreases and stabilizes at the end of the cable release. Additionally, longer cables result in greater variations in pitch angle, a more pronounced overshoot phenomenon, and longer stabilization times. Consequently, the flexure of the tow cable increases with cable length, leading to greater difficulty in controlling and maintaining the morphology of the tow cable, as also confirmed by the study of [73]. This increased flexure further prolongs the time required for outspread. In addition, Li et al. found through experimental studies on a lake with a fixed depth that the increase in cable length affects the increase in drag force on the underwater towing system [74]. Observing Figure 13a, it can be seen that the variation in dry end tension under the same airfoil angle of attack is primarily due to the cable length. In addition, collisions and crossing are frequently observed between cables [75,76]. As shown in Figure 13b by Li et al., it can be observed that the spread of the tow body gradually increases with the length of the cable [74]. Simultaneously, the deflection and deadweight also increase, making spatial attitude control more challenging. This results in greater variation in the spacing between the tow cables, especially near the top, where the nonlinear variation characteristics become more pronounced over time.

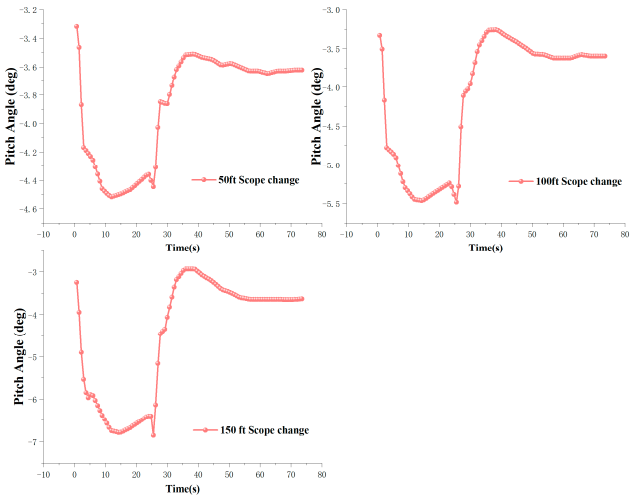

Figure 12. Pitch angle of towed body for various scope changes.

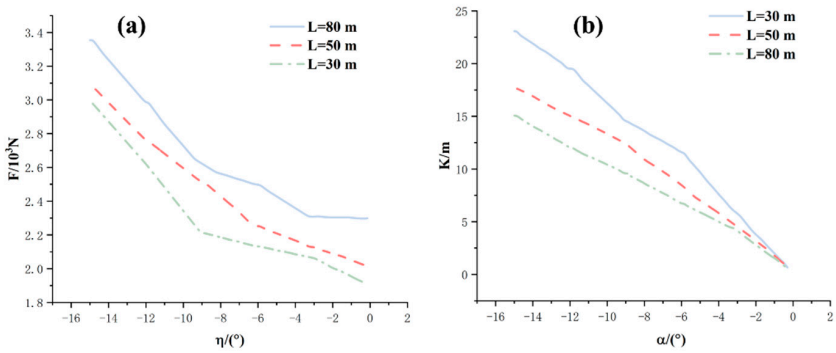

Figure 13. (**a**) Drag force varies with attack angles and cable lengths. (**b**) Spread width varies with attack angles and cable.

4.2. Wave Impact

Waves, as an environmental factor, affect the towing cable array outspread process in the four following ways: wave period [77], wave direction [78], wave height [79], and flow velocity [80] and direction [81].

4.2.1. Wave Period

Based on the structural characteristics of towing cable arrays, it is known that variations in the wave period affect the morphology of the towline during the outspread of multi-branch towing cable arrays. Tang et al. found that the wave period influences the stability of the towing system [82]. As shown in Figure 14 the stability of the system improves with longer wave periods. Kamali and Khojastch conducted a study on the swaying of buoys under two different wave conditions [83]. The motion of the buoy is transmitted to the towline, and some reasonable speculations can be made by examining Figure 15. When the wave period is small, the motion of the buoy is influenced by more frequent and faster waves, resulting in rapid changes in the buoy's motion on the water surface. This frequent motion is transmitted to the attached towline, causing more bends and inflection points as the towline outspread. Conversely, when the wave period is large, the buoy's movement is slower due to the lower frequency of the waves, leading to a smoother trajectory on the water surface. This reduced movement is transmitted to the towline, resulting in fewer bends and inflection points during outspread.

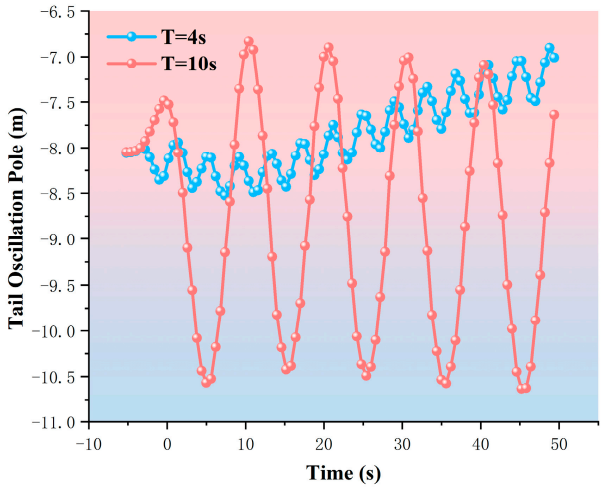

Figure 14. Tail oscillations with wave periods of 10 s and 4 s.

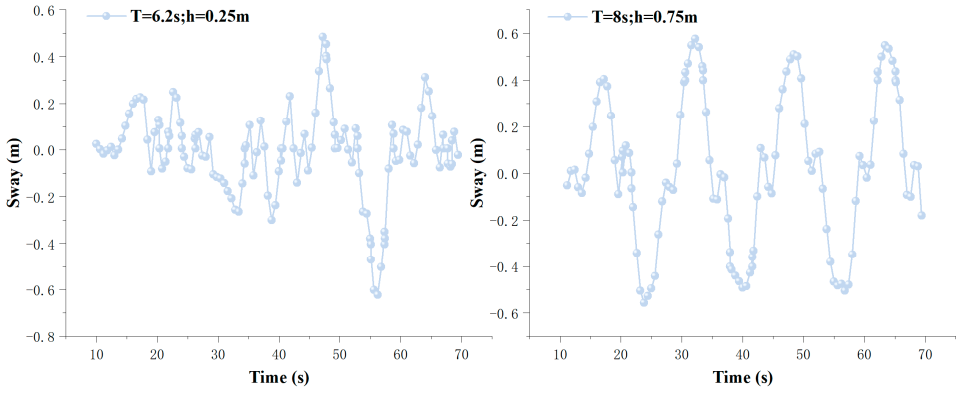

Figure 15. The translational motions of the buoy for two different wave conditions.

It can be seen that when the wave period is too small, the multi-branch towing cable array experiences high-frequency vibrations or may even break into several small segments during outspread. This can cause varying degrees of damage to the sonobuoys and other instruments embedded within the towline. Therefore, it is crucial to select appropriate sea conditions for the outspread of the multi-branch towing cable array, avoiding operations when the wave period is too short.

4.2.2. Wave Direction

The change in wave direction significantly impacts the outspread process of multi-branch towed array systems. Chen studied the characteristics of the tension at the top end of the towed cable under various wave directions. As shown in Figure 16, the tension range at the top end of the towed cable increases as the wave direction shifts from 0° (following the wave) to 180° (against the wave), reaching its maximum at specific wave directions, such as 90° and 180° [84]. The alteration of wave direction affects the outspread process of the multi-branch towed array system. When deploying in the direction of the waves, the process is relatively smooth and steady. However, deploying against or at an angle to the waves makes the process more complex due to the significantly enhanced nonlinear characteristics under these conditions.

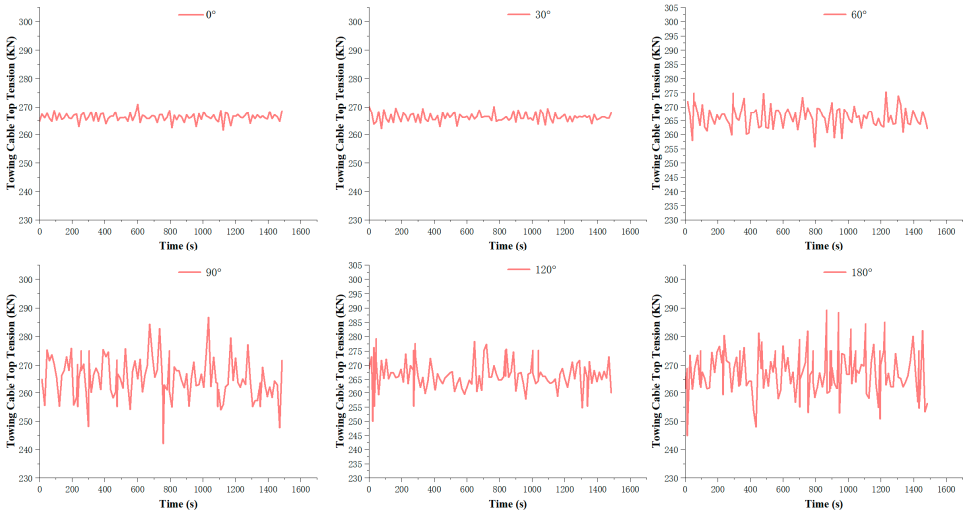

Figure 16. Towing cable top tension in different wave position.

4.2.3. Wave Height

The effect of wave height on the towed line array is investigated by Zhang [85]. By observing Figure 17, it can be seen that the motion varies sinusoidally. Further observation reveals that an increase in wave height leads to an increase in the magnitude of the tug-boat's motion response. This change in wave height alters the boundary conditions of the towline head's motion. Consequently, the enhanced pulling effect on the top of the tow cable significantly amplifies the nonlinear characteristics of the multi-branch towing cable array's outspread process. However, based on the structural characteristics of the towing cable array, an appropriate increase in wave height can positively affect the outspread of the multi-branch line array. This suggests that a moderate increase in wave height can ensure the better utilization of the flexure of the tow cable, facilitating the spreading of the line array.

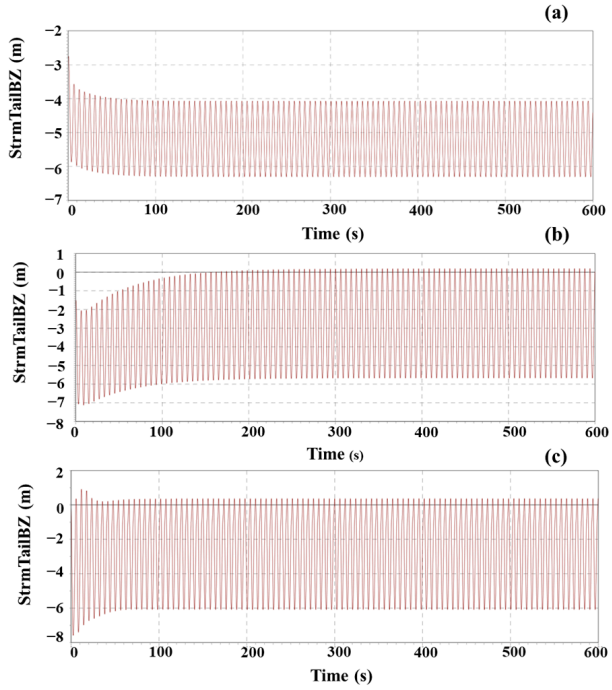

Figure 17. The z-time relationship for the towing cable array. (**a**) H = 2. (**b**) H = 4. (**c**) H = 6 m.

4.2.4. Flow Velocity and Direction

The impact of changes in flow direction and velocity on the outspread process of multi-branch towing cable arrays is significant. Gharib et al. [86] have extensively studied the effects of flow velocity and direction on towing cable arrays. Figure 18 illustrates the geometry of the cable array at various seawater flow rates. When the flow velocity is constant and the angle between the flow direction and the cable axis decreases, the nonlinearity in the cable-array outspread process reduces. Figure 19 shows the tension along the cable array at different seawater flow rates. Higher flow velocities result in increased tensile force, leading to greater nonlinearity in the cable shape. This observation aligns somewhat with the findings in Section 4.1. Figures 20 and 21 depict the arrays at different vessel orientations and constant flow velocities, demonstrating that larger angles correspond to stronger nonlinearity.

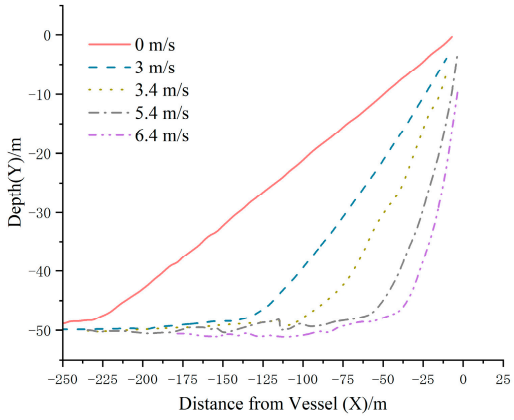

Figure 18. The geometric shape of the cable array in terms of different seawater flow velocities and a constant vessel velocity of 5 m/s for constant array depth.

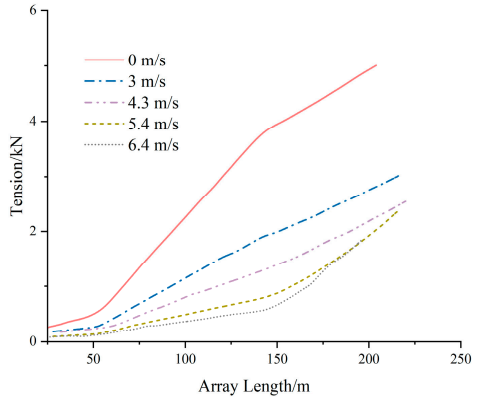

Figure 19. The tension force amount along with the cable array in terms of different seawater flow velocities and a constant vessel velocity of 5 m/s for a constant array depth.

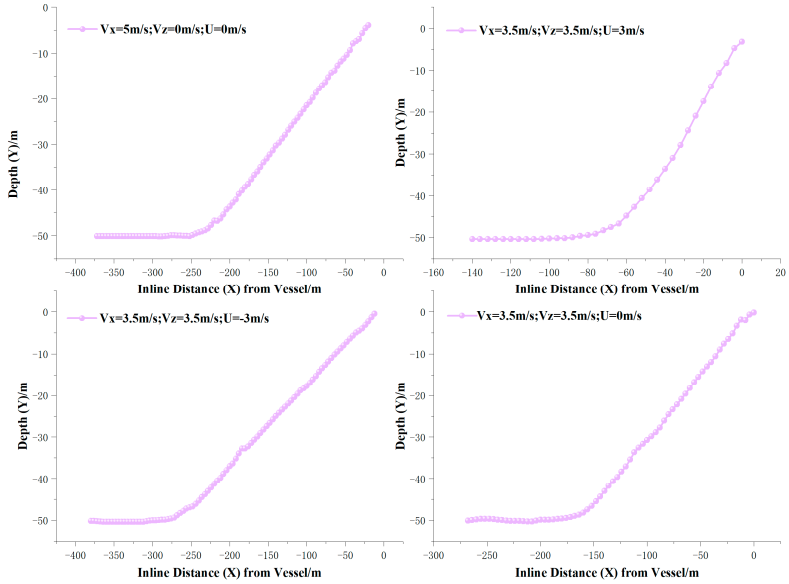

Figure 20. A diagram of the cable array in the direction of sea level according to different seawater velocities and angular vessel motion relative to seawater for a constant depth of the cable array with a vessel velocity of 5 m/s.

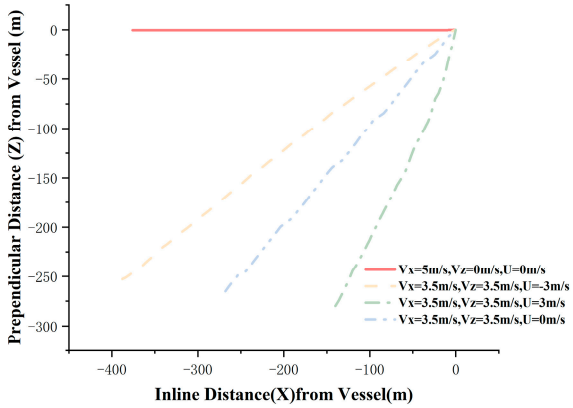

Figure 21. A diagram of the cable array in the direction of depth according to different seawater velocities and angular vessel motion relative to seawater for a constant depth of the cable array with a vessel velocity of 5 m/s.

Therefore, it can be concluded that when the flow velocity is constant, as the angle between the flow direction and the axial direction of the tow cable decreases, the degree of nonlinearity in the outspread process of the cable array also decreases. Conversely, when the flow direction is constant, the degree of nonlinearity in the cable array's spreading increases with rising flow velocity.

Based on the authors' research experience, this phenomenon occurs because as the angle between the flow direction and the axial direction of the tow cable decreases, the obstructive effect of the current on the spreading process of the cable array weakens. Concurrently, the drag effect along the axial direction of the cable array increases, causing the tow cable to straighten. This axial stretching effect diminishes the nonlinearity. When the flow direction is fixed, an increase in flow speed amplifies both the obstructive effect of the current on the spreading process and the drag effect along the axial direction of the cable array, resulting in increased nonlinearity during the spreading process.

4.3. Alignment Spacing

During the outspread of a multi-branch towing cable array, variations in the spacing between the line arrays may result in cable-to-cable collisions, a phenomenon known as cable-to-cable interference [87,88]. A review of the literature on underwater towing systems reveals a primary focus on the interference caused by the seabed [89,90] and other oceanic materials on these systems [91]. These studies have examined the various impacts on marine ecosystems and the seabed caused by the use of towing cable arrays in marine environments. The movement and vibrations of these arrays, particularly through underwater equipment, can disrupt the habitats of marine organisms. Additionally, the towing process may agitate seabed sediments, increasing suspended particles in the water column and thus affecting water quality. Prolonged towing operations may also alter seabed geomorphology and potentially damage the sonar systems of the towing cable arrays.

In contrast, the issue of cable-to-cable interference in towing cable arrays has received little attention. Based on the author's extensive research in the field of underwater towing systems, the interference encountered during the outspread of towed line arrays can be broadly classified into four categories. As illustrated in Figure 22, the four types of interference include self-interference, forward interference, non-forward interference, and multiple interference. Although there are fewer studies on cable-to-cable collisions in the field of towed line arrays, marine cables can, in some cases, exhibit properties similar to flexible rods [92–94]. Consequently, these four types of interference can be briefly analyzed by drawing on studies related to flexible rods [95–99].

Self-interference refers to the phenomenon where a cable experiences coiling due to external forces such as ocean currents, leading to the cable colliding with itself. When the cable coils, it generates significant stress concentrations, especially on the inner side of the bends. This can cause localized fatigue in the cable material, increasing the risk of fracture. During the coiling process, the cable exhibits pronounced nonlinear behavior, particularly during large bends. The combined effects of friction and restorative forces make the cable's movement complex and variable. Forward interference refers to the phenomenon where two cables, or cable-like structures, collide tangentially at their cross-sectional circles. In this type of collision, the tangential contact between the cross-sections of the cables generates significant contact stress, with particularly high normal pressure at the contact points. During contact, relative slippage occurs between the cables, leading to frictional wear at the contact points. This affects the lifespan and reliability of the cables. Non-forward interference refers to the collision that occurs when two cables approach and intersect each other, typically when the spacing between different cable arrays is improperly set. When two cables collide at an intersection, a significant impact force is generated instantaneously. This impact force causes local deformation and stress concentration near the contact points. After the collision, the cables experience vibrational waves along their lengths, which propagate along the cables and affect their overall dynamic response.

Multiple interferences refer to secondary and repeated collisions between cables. This type of collision typically occurs after an initial crossing collision, with subsequent collisions happening due to continued dragging and the influence of ocean currents. After the initial collision, the cables may rebound and flexible waves may propagate, leading to multiple crossing collisions and resulting in a complex dynamic response. Each collision causes some degree of damage and energy loss to the cables. The cumulative effect of multiple collisions can significantly degrade cable performance, potentially leading to failure. Multiple crossing collisions make the cable path very complex and difficult to predict. The cables may undergo numerous turns, bends, and stretches, increasing the system's uncertainty and complexity. Therefore, the spacing between the towing array cables is crucial.

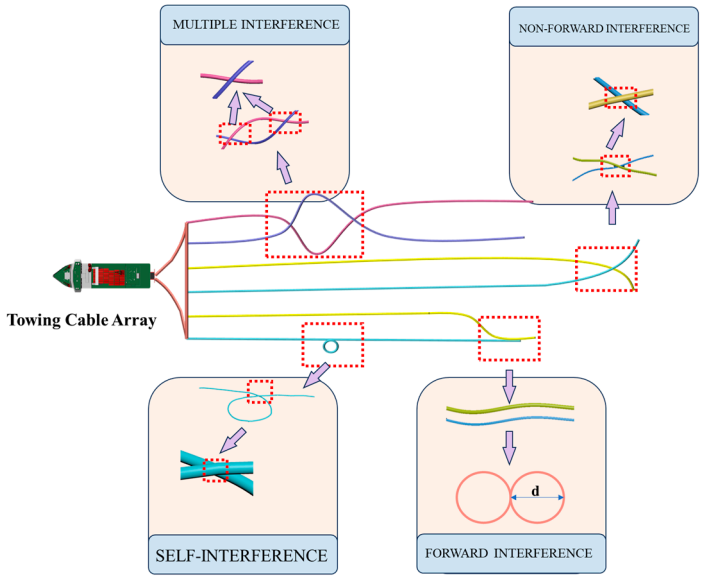

Figure 22. Four different interference scenarios.

In the study [74], it was found that the region with the greatest variation in array spacing is located near a specific length of the cable close to the top end. As wave height and current speed increase, and wave period decreases, this length range shifts towards the tail end. In contrast, the spacing between the rest of the cable's changes little during outspreading. This indicates that during the outspread of a multi-branch towing cable array, the spacing variation between cables is most pronounced near a specific length region close to the top end. In this region, the spacing fluctuates significantly over time, while the relative spacing in other length ranges changes minimally. It can be observed that during the outspread of the towing cable array, there is a jump node in cable spacing at a certain distance from the top end of the cable. The position of this jump node varies with differences in cable length and weight.

4.4. Tip-Drawing Dynamics

Throughout the outspread process of a multi-branch towed array, the top ends of the cables are subjected to strong tensile forces. This is because the lateral outspread makes the forces acting on the top ends of the cables more complex [100,101].

Guo et al. studied the dynamic response frequency characteristics of the towed cable near the ship. As shown in Figure 23, the frequency response near the top end of the towed cable is concentrated due to the pulling action [102]. The outspread of a multi-branch towed-array system primarily relies on the pulling force at the top end. Based on structural characteristics, it can be observed that, due to inertia, parts of the cable farther from the top end bend in the opposite direction. This bending and the bent state change in a very short time, thereby exciting intense vibration waves along the length of the towed cable. The

more severe the external marine environmental loads, the more intense the transmission of these vibrations, which in turn enhances the nonlinearity of the outspread process.

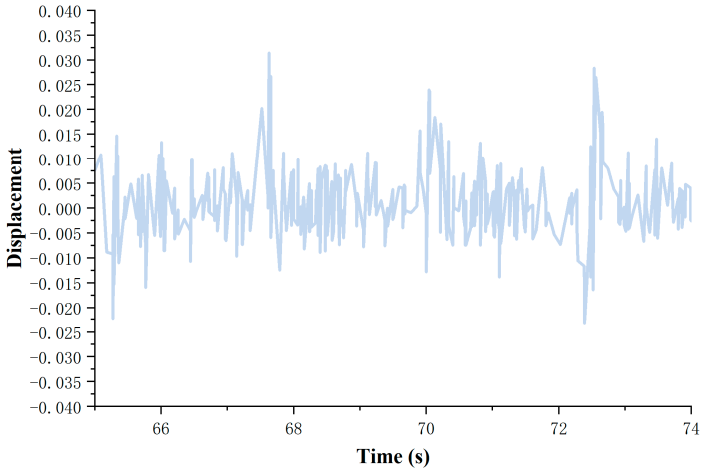

Figure 23. The frequency distribution of the position of the towline near the ship.

4.5. Tension Fluctuations

Chen et al. [103] investigated the tension distribution of towed linear arrays under different tow-cable lengths during the straight navigation of unmanned surface vehicles (USVs). As observed in Figure 24, during the initial stage of outspread, the tension fluctuations at the top of the tow cable are relatively mild. However, as the outspread progresses, these fluctuations at the top of the cable become increasingly severe. This indicates that as the outspread continues, due to the weight and inertia of the tow cable, controlling the tension at the top of the cable becomes more challenging. With the array's further outspread, sharp and significant tension fluctuations at the top become unavoidable. Therefore, to prevent damage to the top of the tow cable, it is necessary to install a tension-buffering device at the top during the outspread of multi-branch towed arrays, to mitigate the severity of the tension fluctuations. Additionally, it can be observed that the transmission of tension fluctuations along the length of the tow cable is not synchronous. The tension stretching effect first acts on the top of the cable, and as it propagates along with the increasing length and ongoing outspread, a whipping effect may occur, leading to a sudden increase in tension at a specific point in the middle of the cable.

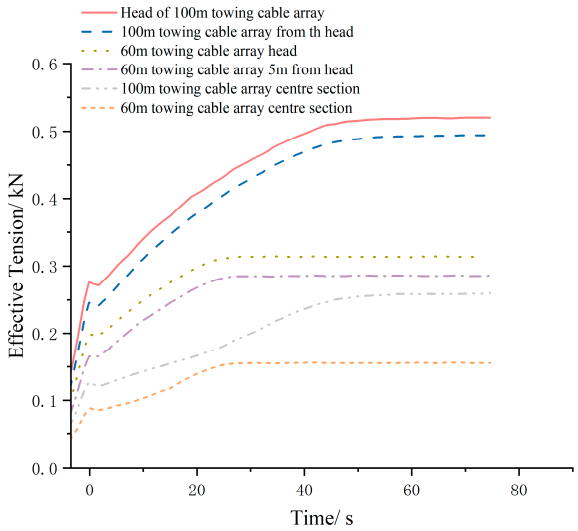

Figure 24. The tension distribution of the towing cable array.

5. The Potential of AI

With the continuous development of computer science and technology, the field of artificial intelligence (AI) has made rapid progress. AI has significantly contributed to scientific research with its powerful capabilities [104–106]. Similarly, AI has been effectively applied in marine engineering research [107–109]. Therefore, AI techniques also have strong potential in the field of towed-line-array outspreading.

5.1. Current Research

Shao et al. utilize Graph Networks (GNs) to enhance the efficiency of iterative solvers in simulating rod dynamics. By predicting the initial guess for the iterative solver, their approach significantly reduces the number of iterations needed to achieve a stable solution, thereby boosting operational efficiency. Additionally, this method ensures long-term stability and maintains the accuracy of the physical system simulation [110].

Zhang et al. developed a tension warning system for underwater towing cables based on a long short-term memory (LSTM) neural network. This system addresses the challenges of monitoring tension in underwater towing cables and the lengthy computation time of time-domain coupled analysis. The study examines the effects of both a single time variable and multiple variables (considering the six degrees of freedom of the tugboat). It predicts and analyzes the time series of tension at critical nodes of the towing cable, comparing these predictions with tension data obtained from numerical simulations using OrcaFlex to validate the accuracy of the predictions [111].

5.2. Application Potential

Artificial intelligence algorithms hold significant potential in the study of the dynamics of the towing cable array deployment process. In this field, various advanced algorithms can be applied to tackle complex problems. Support Vector Machines (SVMs) [112–115] provide powerful tools for addressing dynamic challenges in towing cable arrays, particularly in predictive modeling, the classification of operational states, fault detection, and optimization. Their ability to handle complex, nonlinear data and adapt to changing conditions makes them highly effective in this context. Similarly, Random Forests [116–118], an ensemble machine-learning method based on decision trees, are well-suited for addressing the dynamic behavior and deployment complexities of towing cable arrays. Their effectiveness in handling both classification and regression problems, along with their ability to work with nonlinear and high-dimensional data while providing interpretable results, makes them ideal for this domain.

In underwater and offshore operations, towing cable arrays face dynamic challenges due to varying environmental forces and complex system interactions. Deep Neural Networks (DNNs) [119–121] are used to manage large volumes of nonlinear data and construct precise dynamic models, offering deeper insights into system behaviors. Reinforcement learning algorithms, such as Q-learning [122–124] and Deep Reinforcement Learning (DRL) [125–127], are capable of optimizing real-time control strategies and deployment paths, adapting to dynamically changing environmental conditions. Additionally, data-mining techniques like clustering analysis [128–130] and association rule mining [131–133] uncover latent patterns within the data, supporting system optimization and decision-making processes.

6. Conclusions

This paper systematically reviews the relevant research on the outspread process of multi-branch towing cable arrays and has discovered some intriguing conclusions.

The top of the towing cable array experiences complex pulling forces during the deployment process of a multi-branch towline array. As the length of the array increases, the time required for stabilization after deployment also increases. Greater flexure and a lower natural frequency make attitude control more difficult, resulting in sharp tension fluctuations and potential whiplash effects, with tension often concentrating at the central

node. Wave period and height significantly influence the morphology of the array, as shorter wave periods lead to more bending points and complex shapes, while longer periods result in smoother configurations. The speed and direction of currents also affect the degree of nonlinearity in the array's outspread. The variations in cable spacing are concentrated near the top, with the weight and length of the array influencing the location of jump nodes. As the towline length increases, formation control becomes more challenging, the nonlinear behavior intensifies, and the overall dynamics become more complex.

6.1. Limitations and Challenges

This review provides a valuable summary of the existing research on multi-branch towing cable arrays. However, it highlights several limitations in the current understanding of the outspread dynamics of these arrays. Firstly, most studies have concentrated on the dynamics of towing cable arrays after they have completed the outspread process, with relatively few investigations into the outspread process itself. Additionally, the majority of research has only examined the effects of individual environmental factors on the outspread process, leaving a significant gap regarding the dynamics influenced by multiple concurrent factors.

Furthermore, while some studies draw parallels with parachute opening dynamics, this comparison may overlook critical differences between aerial and underwater towing cable arrays. The review indicates that much research has focused on the interactions between towing cable arrays and the seabed or marine organisms, with insufficient attention given to collisions among the cables themselves.

Despite the rapid development of artificial intelligence technologies, there has been limited application of AI methods in studying towing cable-array dynamics. Moreover, many studies often simplify mathematical models, making assumptions such as uniform water flow and neglecting nonlinear behaviors, which can lead to results that do not accurately represent real-world conditions. The dynamics of towing cable arrays also present multi-scale challenges, ranging from microscopic behaviors at local nodes to macroscopic overall dynamics. Effectively addressing these different scales remains a significant hurdle, and many studies may fall short in this regard.

Lastly, while theoretical and numerical modeling is crucial, the lack of sufficient experimental validation due to the high cost and complexity of underwater experiments can hinder the reliability of these models. Additionally, the structural complexity of towing cable arrays, which includes various components like tow cables, sensor nodes, and connectors, is often inadequately represented in simplified models, potentially failing to capture the dynamic behavior under varying operational conditions. Thus, future research should aim to address these limitations to enhance the understanding of the dynamics of underwater multi-branch towing cable arrays.

6.2. Suggestions and Prospectives

As technology advances, towing cable arrays are expected to expand their applications across various fields, leading to the development of multi-branch towing cable arrays with increasingly complex dynamics. To address the challenges identified in the review, several prospects and suggestions are proposed.

Firstly, it is crucial to conduct economically viable pool experiments or at-sea field trials to gather additional experimental data, which will aid in the validation and calibration of kinetic models. Secondly, developing a multi-scale modeling approach that effectively integrates microscopic local-node mechanical behaviors with macroscopic overall dynamic behaviors will enhance model integrity and accuracy.

Moreover, drawing insights from related research in similar fields can help create more complex nonlinear dynamics models, allowing for a more precise representation of towing-cable-array behavior under diverse operating conditions. It is also essential to incorporate multiple environmental factors—such as currents, temperature, salinity, and

waves—into the dynamics models of towing cable arrays to achieve a more comprehensive understanding of their performance.

The use of artificial intelligence methods for simulating and analyzing the dynamics of the outspread process can provide valuable insights. A detailed investigation into the mechanical mechanisms involved in cable collisions, including aspects like collision forces, deformation, and potential damage, is also necessary. Establishing a comprehensive mechanical model for cable collisions would be fundamental for advancing this area of research.

Additionally, the development and testing of anti-collision devices and technologies, such as cushioning materials between cables, dampers, and active control systems, are essential to mitigate and manage collisions within towing cable arrays. Lastly, conducting uncertainty analyses on environmental factors will enhance the robustness of the models used in studying the dynamic responses of towing cable arrays under varying conditions. Together, these efforts will contribute to a deeper understanding of the complexities associated with multi-branch towline arrays and their dynamics.

Author Contributions: Conceptualization, D.Z.; methodology, D.Z. and Y.L.; investigation, Y.L.; writing—original draft preparation, Y.Z.; data curation, Y.L.; writing—review and editing, D.Z.; formal analysis, Y.M.; visualization, S.Z.; supervision, K.Z.; funding acquisition, Y.L. All authors have read and agreed to the published version of the manuscript.

Funding: The financial support from the Program For Scientific Research Start-Up Funds Of Guangdong Ocean University (R19020) and the Science and Technology Project of Zhanjiang City (2020B01465) to this work is gratefully acknowledged.

Institutional Review Board Statement: Not applicable.

Informed Consent Statement: Not applicable.

Data Availability Statement: Not applicable.

Conflicts of Interest: The authors declare no conflicts of interest.

References

1. Artur, G.; Andrzej, F.; Mariusz, W. Experience with the use of a rigidly-mounted side-scan sonar in a harbour basin bottom investigation. *Ocean Eng.* **2015**, *109*, 439–443. [CrossRef]
2. Letot, L.; Vignand, B. The Forward-Deployed Sonar (FDS) and the Mine Countermeasure Vessel (MCMV). *Nav. Eng. J.* **1994**, *106*, 246–255. [CrossRef]
3. de Moustier, C.; Sotirin, B.J. Performance limitations of hull-mounted sonar arrays in the presence of air bubbles. *J. Acoust. Soc. Am.* **1990**, *88* (Suppl. S1), S131–S132. [CrossRef]
4. Reif, B.A.P.; Andreassen, Ø. The Impact of Flow Noise on Towed and Hull Mounted Acoustical Sensors: An Introductory Study. 2004. Available online: https://www.ffi.no/en/publications-archive/the-impact-of-flow-noise-on-towed-and-hull-mounted-acoustical-sensors-an-introductory-study (accessed on 28 January 2024).
5. Zhang, D.; Zhao, B.; Zhu, K. Hydrodynamic response of ocean-towed cable-array system under different munk moment coefficients. *Sustainability* **2022**, *14*, 1932. [CrossRef]
6. Zhang, D.; Zhao, B.; Yang, Y.; Zhu, K.; Jiang, H. Numerical Modelling and Dynamic Analysis of Ocean Towed Cable-array System Under Munk Moment During Turning Maneuver. Available online: http://univpubl.com/public/uploads/20240416/1d3a8f01f3b355724036d376760ccae5.pdf (accessed on 10 June 2024).
7. Northardt, T. Observability criteron guidance for passive towed array sonar tracking. *IEEE Trans. Aerosp. Electron. Syst.* **2022**, *58*, 3578–3585. [CrossRef]
8. Liu, Y.; Cheng, L.; Zou, Y.; Hu, Z. Thin Fiber-Optic Hydrophone Towed Array for Autonomous Underwater Vehicle. *IEEE Sensors J.* **2024**, *24*, 15125–15132. [CrossRef]
9. Li, J.; Pei, Y.; Liu, C.; Zhang, L.; Luo, X.; Liu, K.; Li, W. A robust array geometry inversion method for a deep-towed multichannel seismic system with a complex seafloor. *Front. Mar. Sci.* **2023**, *10*, 1283061. [CrossRef]
10. Mayer, L.A. Frontiers in seafloor map** and visualization. *Mar. Geophys. Res.* **2006**, *27*, 7–17. [CrossRef]
11. Karl, H.A.; Schwab, W.C.; Wright, A.S.C.; Drake, D.E.; Chin, J.L.; Danforth, W.W.; Ueber, E. Acoustic map** as an environmental management tool: I. Detection of barrels of low-level radioactive waste, Gulf of the Farallones National Marine Sanctuary, California. *Ocean Coast. Manag.* **1994**, *22*, 201–227. [CrossRef]

12. Sakagami, N.; Hirayama, K.; Taba, R.; Kobashigawa, S.; Arashiro, S.; Takemura, F.; Takahashi, S. Development of a towed optical camera array system (SSS: Speedy Sea Scanner) for sea environmental monitoring. In Proceedings of the 2018 OCEANS-MTS/IEEE Kobe Techno-Oceans (OTO), Kobe, Japan, 28–31 May 2018; IEEE: New York, NY, USA, 2018.
13. von Benda-Beckmann, A.M.; Beerens, S.P.; van Ijsselmuide, S.P. Van Ijsselmuide. Effect of towed array stability on instantaneous localization of marine mammals. *J. Acoust. Soc. Am.* **2013**, *134*, 2409–2417. [CrossRef]
14. Thode, A. Tracking sperm whale (Physeter macrocephalus) dive profiles using a towed passive acoustic array. *J. Acoust. Soc. Am.* **2004**, *116*, 245–253. [CrossRef] [PubMed]
15. Birin, I.; Maglić, L. Analysis of seismic methods used for subsea hydrocarbon exploration. *Pomor. Zb.* **2020**, *58*, 77–89. [CrossRef]
16. Dosso, S.E.; Riedel, M. Array element localization for towed marine seismic arrays. *J. Acoust. Soc. Am.* **2001**, *110*, 955–966. [CrossRef]
17. Bjørnø, L. Developments in sonar and array technologies. In Proceedings of the 2011 IEEE Symposium on Underwater Technology and Workshop on Scientific Use of Submarine Cables and Related Technologies, Tokyo, Japan, 5–8 April 2011; IEEE: New York, NY, USA, 2011.
18. Ødegård, Ø.; Sørensen, A.J.; Hansen, R.E.; Ludvigsen, M. A new method for underwater archaeological surveying using sensors and unmanned platforms. *IFAC-Pap.* **2016**, *49*, 486–493. [CrossRef]
19. Ambatt, S.K. Fault Detection and Prognostic Health Monitoring of Towed Array Sonars. *Def. Sci. J.* **2022**, *72*, 495–503.
20. Zhang, D.; Zhang, Y.; Zhao, B.; Ma, Y.; Si, K. Exploring Subsea Dynamics: A Comprehensive Review of Underwater Pipelines and Cables. *Phys. Fluids* **2024**, *36*, 101304. [CrossRef]
21. Eleftherakis, D.; Vicen-Bueno, R. Sensors to increase the security of underwater communication cables: A review of underwater monitoring sensors. *Sensors* **2020**, *20*, 737. [CrossRef]
22. Norris, M.; Oppenheim, C. Comparing alternatives to the Web of Science for coverage of the social sciences' literature. *J. Informetr.* **2007**, *1*, 161–169. [CrossRef]
23. Zhang, D.; Zhao, B.; Sun, J.; Zhang, Y.; Zhu, K.; Jiang, H. Influence of Different Static Equilibrium Calculation Methods on the Dynamic Response of Marine Cables during the Releasing Process: Review and a Case Study. *J. Mar. Sci. Eng.* **2023**, *11*, 764. [CrossRef]
24. Zhang, D.; Zhao, B.; Zhu, K. Mechanical characteristics analysis of horizontal lifting of subsea pipeline with different burial depths. *Front. Earth Sci.* **2022**, *10*, 1011291. [CrossRef]
25. Zhang, D.; Zhao, B.; Zhu, K. Dynamic Analysis of Pipeline Lifting Operations for Different Current Velocities and Wave Heights. *FDMP-Fluid Dyn. Mater. Process.* **2022**, *19*, 603–617. [CrossRef]
26. Zhang, D.; Zhao, B.; Zhu, K. Dynamic analysis of the umbilical cable pull-in operation through J-tube under different wave directions. *Ocean Eng.* **2023**, *280*, 114838. [CrossRef]
27. Hong, C.A.O.; Jian, Y.U.; Yaru, C.H.A.N.G.; Yue, L.I. Visualization analysis of the hotspots and trend of researches on fracture liaison service based on CiteSpace. *Tianjin J. Nurs.* **2023**, *31*, 554.
28. Hu, H.; Xue, W.; Jiang, P.; Li, Y. Bibliometric analysis for ocean renewable energy: An comprehensive review for hotspots, frontiers, and emerging trends. *Renew. Sustain. Energy Rev.* **2022**, *167*, 112739. [CrossRef]
29. Ma, Y.; Zhang, D.; Zhang, Y.; Zhao, G.; Xie, Y.; Jiang, H. Advancements and Challenges in Deep Learning-Driven Marine Data Assimilation: A Comprehensive Review. *Comput. Res. Prog. Appl. Sci. Eng.* **2023**, *9*, 1–17. [CrossRef]
30. Lai, Q.; Ma, J.; He, F.; Zhang, A.; Pei, D.; Wei, G.; Zhu, X. Research development, current hotspots, and future directions of blue carbon: A bibliometric analysis. *Water* **2022**, *14*, 1193. [CrossRef]
31. Lan, T.; Wang, Y.; Qiu, L.; Liu, G. Array shape estimation based on tug vehicle noise for towed linear array sonar during turning. *Ocean Eng.* **2024**, *303*, 117554. [CrossRef]
32. Liu, J.; Gao, S.; Nian, R.; He, B.; Yan, T. Study on hydrodynamic characteristics and depth control of the towed sensors array system. *Mar. Struct.* **2023**, *92*, 103504. [CrossRef]
33. Zhang, D.; Zhao, B.; Zhu, K.; Jiang, H. Dynamic analysis of towed cable with variable length during turning maneuvers. *Sci. Rep.* **2023**, *13*, 3525. [CrossRef]
34. Antony, T.; Adithya, P.V.; Madhusoodanan, K.N.; Kumar, K.R. Miniature fiber optic towed array for AUV applications. In *Global Oceans 2020: Singapore–US Gulf Coast*; IEEE: New York, NY, USA, 2020.
35. Park, S.H.; Lee, S.J.; Lee, S. Experimental investigation of towing-and course-stability of a FPSO towed by a tug-boat with lateral motion. *Int. J. Nav. Archit. Ocean Eng.* **2021**, *13*, 12–23. [CrossRef]
36. Yang, D.; Feng, Z.; Huang, H.; Zhang, Q.; Yang, T. Aerodynamic simulation and analysis of large ring-sail parachute. *J. Phys. Conf. Ser. Vol.* **2022**, *2383*, 012078. [CrossRef]
37. Eiden, M.J.; Foster, W.A. Parachute system design. In *Safety Design for Space Systems*; Butterworth-Heinemann: Oxford, UK, 2023; pp. 377–399.
38. Ray, E.; Samuel, A.J. Orion Main Parachute Asymmetry Testing Revisited. In Proceedings of the 26th AIAA Aerodynamic Decelerator Systems Technology Conference, Toulouse, France, 16–19 May 2022.
39. Mattei, M.; Phillippe, C.; Panerai, F.; Villafañe Roca, L. Design, manufacturing, and testing of sub-scale flat and conical parachutes. In Proceedings of the AIAA SCITECH 2023 Forum, National Harbor, MD, USA, 23–27 January 2023.
40. Ray, E. Reefing line tension in CPAS main parachute clusters. In Proceedings of the AIAA Aerodynamic Decelerator Systems (ADS) Conference, Daytona Beach, FL, USA, 26 March 2013.

41. Zhao, B.; Zhang, D.; Zhu, K. Lifting of horizontal subsea pipeline with diverse lifting points in waves: Hydrodynamic analysis. *Phys. Fluids* **2024**, *36*, 8. [CrossRef]
42. Zhang, D.; Bai, Y.; Jing, B.; Zhu, K.; Sun, G. Motion simulation analysis of the cable-body of the deep underwater towed system. In Proceedings of the ASME 2018 37th International Conference on Ocean, Offshore and Arctic Engineering, Madrid, Spain, 17–22 June 2018.
43. Zhang, D.; Zhao, B.; Zhu, K.; Jiang, H. Dynamic analysis of the subsea production system with lazy-wave risers attached to FPSO. *PLoS ONE* **2023**, *18*, e0291603. [CrossRef]
44. Zhu, K.; Li, D.; Li, W. Time-domain analysis of unified agglutination parameters for marine cable systems. *Ocean Eng.* **2002**, *2*, 100–104. (In Chinese) [CrossRef]
45. Zhu, K.Q.; Li, D.G.; Feng, S.; Li, W.Y. A parameter studying method on mooring towing and submersible umbilical cables. *J. East China Shipbuild. Institude (Nat. Sci. Ed.)* **2003**, *17*, 1–5.
46. Gu, J.; Wang, Z. Influence of Vehicle Wake on the Control of Towed Systems. *Appl. Sci.* **2024**, *14*, 4944. [CrossRef]
47. Zhang, D.; Zhang, T.; Zhu, K.; Bai, Y.; Liu, J. *Application of OrcaFlex in Dynamic Simulation of Offshore Engineering and Submarine Pipelines*; Zhejiang University Press: Hangzhou, China, 2019. (In Chinese)
48. Singh, R.K.; Subrata, K.; Shovan, B. Dynamics of a Towed Cable with Sensor-Array for Underwater Target Motion Analysis. *arXiv* **2024**, arXiv:2405.05937.
49. Lee, D.H.; Huynh, T.; Kim, Y.B.; Park, J.S. Motion control system design for Barge-Type surface ships using Tugboats. *J. Mar. Sci. Eng.* **2022**, *10*, 1413. [CrossRef]
50. Li, O.; Zhou, Y. Precise trajectory tracking control of ship towing systems via a dynamical tracking target. *Mathematics* **2021**, *9*, 974. [CrossRef]
51. Zhu, H.; Hu, C. A unified seakee** and maneuvering analysis of multiple linked towing system with triangular Bodies. *Ocean Eng.* **2021**, *222*, 108577. [CrossRef]
52. Yang, X.; Wu, J.; Xu, S. Dynamic analysis of underwater towed system under undulating motion mode of towed vehicle. *Appl. Ocean Res.* **2022**, *121*, 103083. [CrossRef]
53. Grindheim, J.V.; Revhaug, I.; Pedersen, E.; Solheim, P. Modeling, prediction and control of towed marine seismic streamers. *Kart Og Plan* **2017**, *77*, 1–16.
54. Grindheim, J.V.; Revhaug, I.; Pedersen, E.; Solheim, P. A Simplified Solution to the Negative Tension Problem of a Three Dimensional Towed Underwater Cable Model. 2018. Available online: https://proceedings.science/sobena-congresso/sobena-2018/trabalhos/a-simplified-solution-to-the-negative-tension-problem-of-a-three-dimensional-tow?lang=pt-br (accessed on 5 May 2024).
55. Yang, B.; Zhu, K.; Zhu, Y.; Qin, D. Dynamic response of towed line array. *J. Hydrodyn.* **2013**, *25*, 616–619. [CrossRef]
56. Karimirad, M.; Torgeir, M. Wave-and wind-induced dynamic response of a spar-type offshore wind turbine. *J. Waterw. Port Coast. Ocean Eng.* **2012**, *138*, 9–20. [CrossRef]
57. Moan, T.; Zheng, X.Y. Quasi-static response of fixed offshore platforms to Morison-type wave loadings. *J. Eng. Mech.* **2009**, *135*, 1057–1068. [CrossRef]
58. Zhang, D.; Bai, Y.; Soares, C.G. Dynamic analysis of an array of semi-rigid sea station fish cages subjected to waves. *Aquac. Eng.* **2021**, *94*, 102172. [CrossRef]
59. Driscoll, F.; Lueck, R.; Nahon, M. The motion of a deep-sea remotely operated vehicle system: Part 1: Motion observations. *Ocean Eng.* **2000**, *27*, 29–56. [CrossRef]
60. Yang, S.; Zhu, X.; Ren, H. Dynamic analysis of a deep-towed seismic system based on a flexible multi-body dynamics frame. *Ocean Eng.* **2023**, *279*, 114587. [CrossRef]
61. French, K.E. Inflation of a Parachute. *AIAA J.* **1963**, *1*, 2615–2617. [CrossRef]
62. Morris, A.; Olson, L.; Taylor, T. Load asymmetry observed during orion main parachute inflation. In Proceedings of the 21st AIAA Aerodynamic Decelerator Systems Technology Conference and Seminar, Dublin, Ireland, 23–26 May 2011.
63. Potvin, J.; Peek, G.; Brocato, B. Modeling the Inflation of ram-air Parachutes reefed with Sliders. *J. Aircr.* **2001**, *38*, 818–827. [CrossRef]
64. Zhang, M.; Gao, P. Study on Line Sail in the Process of Double-guided Parachute Deployment. *IOP Conf. Ser. Earth Environ. Sci.* **2019**, *295*, 042101. [CrossRef]
65. Purvis, J. Improved prediction of parachute line sail during lines-first deployment. In Proceedings of the 8th Aerodynamic Decelerator and Balloon Technology Conference, Hyannis, MA, USA, 2–4 April 1984.
66. Zhang, Q. A new parachute deployment model by multibody dynamics. In Proceedings of the 17th AIAA Aerodynamic Decelerator Systems Technology Conference and Seminar, Monterey, CA, USA, 19–22 May 2003.
67. Wang, H. Dynamic modeling and simulation of whip** phenomenon for large parachute. *AIAA J.* **2018**, *56*, 4049–4059. [CrossRef]
68. Chapman, D.A. Towed cable behaviour during ship turning manoeuvers. *Ocean Eng.* **1984**, *11*, 327–361. [CrossRef]
69. Grosenbaugh, M.A. Transient behavior of towed cable systems during ship turning maneuvers. *Ocean Eng.* **2007**, *34*, 1532–1542. [CrossRef]
70. Wang, Z.; Sun, G. Parameters influence on maneuvered towed cable system dynamics. *Appl. Ocean Res.* **2015**, *49*, 27–41. [CrossRef]
71. Mudie, J.D.; Ivers, W.D. Simulation studies of the response of deeply towed vehicle to various towing ship maneuvers. *Ocean Eng.* **1975**, *3*, 37–46. [CrossRef]

72. Kamman, J.W.; Huston, R.L. Modeling of variable length towed and tethered cable systems. *J. Guid. Control Dyn.* **1999**, *22*, 602–608. [CrossRef]
73. Grosenbaugh, M.A. *Dynamic Behavior of Towed Cable Systems During Ship Turning Maneuvers*; Woods Hole Oceanographic Institution: Falmouth, MA, USA, 2005.
74. Li, C.; Ai, Y.; Yu, H.; Jiang, X.; Song, W.; Wang, M. Lake experimental study on depth determination and deployment performance of underwater towing system. *J. Harbin Eng. Univ.* **2022**, *43*, 62–68. (In Chinese)
75. Pipchenko, A.; Tsymbal, N. Development of Mathematical Algorithms for the Seismic Research Vessel Maneuvering Simulator. Proceedings of the INSLC. Available online: https://www.researchgate.net/profile/Oleksandr-Pipchenko/publication/336798657_Development_of_Mathematical_Algorithms_for_the_Seismic_Research_Vessel_Maneuvering_Simulator/links/5ec29f52a6fdcc90d67e2fc7/Development-of-Mathematical-Algorithms-for-the-Seismic-Research-Vessel-Maneuvering-Simulator.pdf (accessed on 5 May 2024).
76. Obligado, M.; Bourgoin, M. An experimental investigation of the equilibrium and stability of long towed cable systems. *New J. Phys.* **2013**, *15*, 043019. [CrossRef]
77. Cahill, B.; Lewis, T. Wave Periods and the Calculation of Wave Power. 2014. Available online: http://hdl.handle.net/10919/49206 (accessed on 4 April 2024).
78. Steele, K.; Teng, C.-C.; Wang, D. Wave direction measurements using pitch-roll buoys. *Ocean Eng.* **1992**, *19*, 349–375. [CrossRef]
79. Lauria, A.; Loprieno, P.; Rizzo, F.; Severini, A.; Foti, D.; Leone, E.; Francone, A.; Tomasicchio, G. On the effects of wind and operating conditions on mooring line tensions for floating offshore wind turbine. *Appl. Ocean Res.* **2024**, *152*, 104197. [CrossRef]
80. Chagnaud, B.P.; Brücker, C.; Hofmann, M.H.; Bleckmann, H. Measuring flow velocity and flow direction by spatial and temporal analysis of flow fluctuations. *J. Neurosci.* **2008**, *28*, 4479–4487. [CrossRef] [PubMed]
81. Constantin, A.; University of Vienna; Johnson, R. Steady large-scale ocean flows in spherical coordinates. *Oceanography* **2018**, *31*, 42–50. [CrossRef]
82. Tang Zh Zhu, K.; Bao, X. Study on the tension of the towing section and the vibration extreme value of the tail rope segment in the multi-branch towing line array system. *J. Ningbo Univ. (Sci. Eng.)* **2016**, *29*, 127–132. (In Chinese)
83. Kamali, R.; Danial, K. Investigation of dynamic behavior of a towed underwater vehicle at Persian Gulf. In Proceedings of the 24th Annual International Conference on Mechanical Engineering-ISME, Yazd, Iran, 26–28 April 2016.
84. Chen, S. The Research for Motion Response Analysis of Towed Linear Array Sonar. Master's Thesis, Dalian University of Technology, Dalian, China, 2021. (In Chinese).
85. Zhang, Y. Numerical Study on the Nonlinear Hydrodynamic Characteristics of Towed Linear Array Sonar. Master's Thesis, Ningbo University, Ningbo, China, 2015. (In Chinese)
86. Gharib, M.R.; Heydari, A.; Kolahi, M.R.S. Modeling and analysis of static and dynamic behavior of marine towed cable-array system based on the vessel motion. *Adv. Mech. Eng.* **2024**, *16*, 16878132231220353. [CrossRef]
87. Bai, Y.; Zhang, D.; Zhu, K.; Zhang, T. Dynamic analysis of umbilical cable under interference with riser. *Ships Offshore Struct.* **2018**, *13*, 809–821. [CrossRef]
88. Guo, Y.; Li, P.; Qin, H.; Jiang, Z. Research on the Influence of Seabed on the Hydrodynamic Performance of the Underwater Vehicle. In Proceedings of the ISOPE International Ocean and Polar Engineering Conference, ISOPE, Shanghai, China, 5–10 June 2022.
89. Asmael, M.; Amin, M. A review on recent achievements and challenges in electrochemical machining of tungsten carbide. *Arch. Adv. Eng. Sci.* **2024**, *2*, 1–23. [CrossRef]
90. Thorleifson, J.M.; Davies, T.C.; Black, M.R.; Hopkin, D.A.; Verrall, R.I.; Pope, A. The Theseus autonomous underwater vehicle. A Canadian success story. In Proceedings of the Oceans' 97. MTS/IEEE Conference Proceedings, Halifax, NS, Canada, 6–9 October 1997; IEEE: New York, NY, USA, 1997; Volume 2.
91. Blintsov, V.S.; Trunin, K.S.; Tarełko, W. Determination of additional tension in towed streamer cable triggered by collision with underwater moving object. *Pol. Marit. Res.* **2020**, *2*, 58–68. [CrossRef]
92. Wang, F.; Tu, W.; Deng, D.; Wu, X. Dynamic effect research of cable-lead-in rod on towed system. *J. Shanghai Jiaotong Univ. (Sci.)* **2019**, *24*, 745–753. [CrossRef]
93. Liu, C.; Zhang, Y.; Yuan, X. Simulation of Recycling Cable in Underwater Towed System. In Proceedings of the 1st International Conference on Mechanical Engineering and Material Science (MEMS 2012), Shanghai, China, 28–30 December 2012; Atlantis Press: Amsterdam, The Netherlands, 2012.
94. Ivanovskaya, A.V.; Bogatyreva, E.V.; Rybak, A.T. Simulation of the cable part of the load-lifting device drive, represented as a rod system. *IOP Conf. Ser. Mater. Sci. Eng.* **2020**, *1001*, 012059. [CrossRef]
95. Wang, W. Research on the Dynamic Substructure Method of Transient Response of Multiple Collisions of Flexible Beam-Rod Structures. Ph.D. Dissertation, Nanjing University of Science and Technology, Nanjing, China, 2014. (In Chinese)
96. Gu, T. Rigid-Flexible Coupling Flexible Manipulator Collision Dynamics. Master's Thesis, Jiangsu University of Science and Technology, Jiangsu, China, 2021. (In Chinese) [CrossRef]
97. Qian, Z. Rigid-Flexible Coupling Flexible Manipulator with Friction Collision Dynamics. Ph.D. Dissertation, Nanjing University of Science and Technology, Nanjing, China, 2016. (In Chinese).
98. Yang, Y.; Feng, H.; Chen, H.; Wu, M. Analysis of oblique collision characteristics of flexible rod and cam. *Acta Phys. Sin.* **2016**, *65*, 40–46. (In Chinese)

99. Huang, Y.B. General Relationship between kinetic energy loss and recovery coefficient in collision and its proof. *Phys. Eng.* **2020**, *30*, 39–44. (In Chinese)
100. Zhang, D.; Zhu, K.; Li, Y.; Yan, X.; Ji, F. Dynamics analysis of the slewing process of a multi-branched towline array under the combined action of wave currents. *Ship Eng.* **2015**, *37*, 86–92. (In Chinese) [CrossRef]
101. Mao, Y. Effect of waterfowl parameters on the dynamic response of a multi-branched towline array. *J. Appl. Mech.* **2018**, *35*, 254–260+447. (In Chinese)
102. Guo, L.; Yuan, Y.; Tang, W.; Xue, H. A numerical investigation on quasi-static configuration and nonlinear dynamic response characteristics of marine towing cable. *Ocean Eng.* **2021**, *240*, 110007. [CrossRef]
103. Chen, D.-D.; Li, W.; Bao, X.; Zhu, K. Research on obstacle avoidance method for surface unmanned craft with towed line array. *J. Huazhong Univ. Sci. Technol. (Nat. Sci. Ed.)* **2020**, *48*, 72–77. (In Chinese) [CrossRef]
104. Mpia, H.N.; Syasimwa, L.M.; Muyisa, D.M. Comparative Machine Learning Models for Predicting Loan Fructification in a Semi-Urban Area. *Arch. Adv. Eng. Sci.* **2024**, 1–12. [CrossRef]
105. Van Noorden, R.; Jeffrey, M.P. AI and science: What 1600 researchers think. *Nature* **2023**, *621*, 672–675. [CrossRef]
106. Himanen, L.; Geurts, A.; Foster, A.S.; Rinke, P. Data-driven materials science: Status, challenges, and perspectives. *Adv. Sci.* **2019**, *6*, 1900808. [CrossRef]
107. Zhang, Y.; Zhang, D.; Jiang, H. A review of artificial intelligence-based optimization applications in traditional active maritime collision avoidance. *Sustainability* **2023**, *15*, 13384. [CrossRef]
108. Zhang, Y.; Zhang, D.; Jiang, H. Review of challenges and opportunities in turbulence modeling: A comparative analysis of data-driven machine learning approaches. *J. Mar. Sci. Eng.* **2023**, *11*, 1440. [CrossRef]
109. Zhang, D.; Ma, Y.; Zhang, H.; Zhang, Y. Marine Equipment Siting Using Machine-Learning-Based Ocean Remote Sensing Data: Current Status and Future Prospects. *Sustainability* **2024**, *16*, 8889. [CrossRef]
110. Shao, H.; Kugelstadt, T.; Hadrich, T.; Pałubicki, W.; Bender, J.; Pirk, S.; Michels, D.L. Accurately solving rod dynamics with graph learning. *Adv. Neural Inf. Process. Syst.* **2021**, *34*, 4829–4842.
111. Zhang, X.; Dong, L.; Zhang, Q.; He, W.; Sun, J.; Li, X. Prediction of underwater towing cable tension based on LSTM neural network. In Proceedings of the Fourth International Conference on Artificial Intelligence and Electromechanical Automation (AIEA 2023), Nanjing, China, 10–12 March 2023; SPIE: Ogden, UT, USA, 2023; Volume 12709.
112. Hearst, M.A.; Dumais, S.T.; Osuna, E.; Platt, J.; Scholkopf, B. Support vector machines. *IEEE Intell. Syst. Their Appl.* **1998**, *13*, 18–28. [CrossRef]
113. Steinwart, I.; Andreas, C. *Support Vector Machines*; Springer Science & Business Media: Berlin/Heidelberg, Germany, 2008.
114. Meyer, D. Support vector machines. *R News* **2001**, *1*, 23–26.
115. Kecman, V. Support vector machines–an introduction. In *Support Vector Machines: Theory and Applications*; Springer: Berlin/Heidelberg, Germany, 2005; pp. 1–47.
116. Breiman, L. Random forests. *Mach. Learn.* **2001**, *45*, 5–32. [CrossRef]
117. Hastie, T.; Tibshirani, R.; Friedman, J. *The Elements of Statistical Learning: Data Mining, Inference, and Prediction*; Springer: New York, NY, USA, 2009; Volume 2.
118. Cutler, A.D.; Richard, C.; John, R.S. Random forests. In *Ensemble Machine Learning: Methods and Applications*; Springer: Berlin/Heidelberg, Germany, 2012; pp. 157–175.
119. Sze, V.; Chen, Y.-H.; Yang, T.-J.; Emer, J.S. Efficient processing of deep neural networks: A tutorial and survey. *Proc. IEEE* **2017**, *105*, 2295–2329. [CrossRef]
120. Larochelle, H.; Bengio, Y.; Louradour, J.; Lamblin, P. Exploring strategies for training deep neural networks. *J. Mach. Learn. Res.* **2009**, *10*, 1–40.
121. Szegedy, C.; Toshev, A.; Erhan, D. Deep neural networks for object detection. In *Advances in Neural Information Processing Systems*; MIT Press: Cambridge, MA, USA, 2013; p. 26.
122. Watkins, C.J.; Dayan, P. Q-learning. *Mach. Learn.* **1992**, *8*, 279–292. [CrossRef]
123. Clifton, J.; Eric, L. Q-learning: Theory and applications. *Annu. Rev. Stat. Its Appl.* **2020**, *7*, 279–301. [CrossRef]
124. Fan, J.; Wang, Z.; Xie, Y.; Yang, Z. A theoretical analysis of deep Q-learning. In *Learning for Dynamics and Control*; PMLR: New York, NY, USA, 2020.
125. Li, Y. Deep reinforcement learning: An overview. *arXiv* **2017**, arXiv:1701.07274.
126. Arulkumaran, K.; Deisenroth, M.P.; Brundage, M.; Bharath, A.A. Deep reinforcement learning: A brief survey. *IEEE Signal Process. Mag.* **2017**, *34*, 26–38. [CrossRef]
127. Sewak, M. *Deep Reinforcement Learning*; Springer: Singapore, 2019.
128. Diday, E.; Simon, J.C. Clustering analysis. In *Digital Pattern Recognition*; Springer: Berlin/Heidelberg, Germany, 1976; pp. 47–94.
129. Garcia-dias, R.; Vieira, S.; Pinaya, W.H.L.; Mechelli, A. Clustering analysis. In *Machine Learning*; Academic Press: Cambridge, MA, USA, 2020; pp. 227–247.
130. Lee, R.C.T. Clustering analysis and its applications. In *Advances in Information Systems Science*; Springer: Boston, MA, USA, 1981; Volume 8, pp. 169–292.
131. Liao, S.-H.; Chu, P.-H.; Hsiao, P.-Y. Data mining techniques and applications—A decade review from 2000 to 2011. *Expert Syst. Appl.* **2012**, *39*, 11303–11311. [CrossRef]

132. Olson, D.L.; Dursun, D. *Advanced Data Mining Techniques*; Springer Science & Business Media: New York, NY, USA, 2008.
133. Pujari, A.K. *Data Mining Techniques*; Universities Press: Madison, CT, USA, 2001.